

STATISTICAL MECHANICS FOR COMPLEXITY

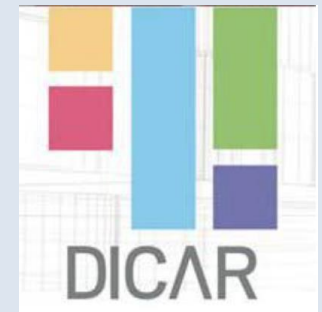
A CELEBRATION OF THE 80TH BIRTHDAY OF CONSTANTINO TSALLIS

RIO DE JANEIRO, 6 TO 10 NOVEMBER 2023

THE APPLICATION OF Q-STATISTICS TO ACOUSTIC EMISSIONS OF COMPRESSED CONSTRUCTION MATERIALS APPROACHING FAILURE



Annalisa Greco
Department of Civil Engineering and Architecture
University of Catania (Italy)



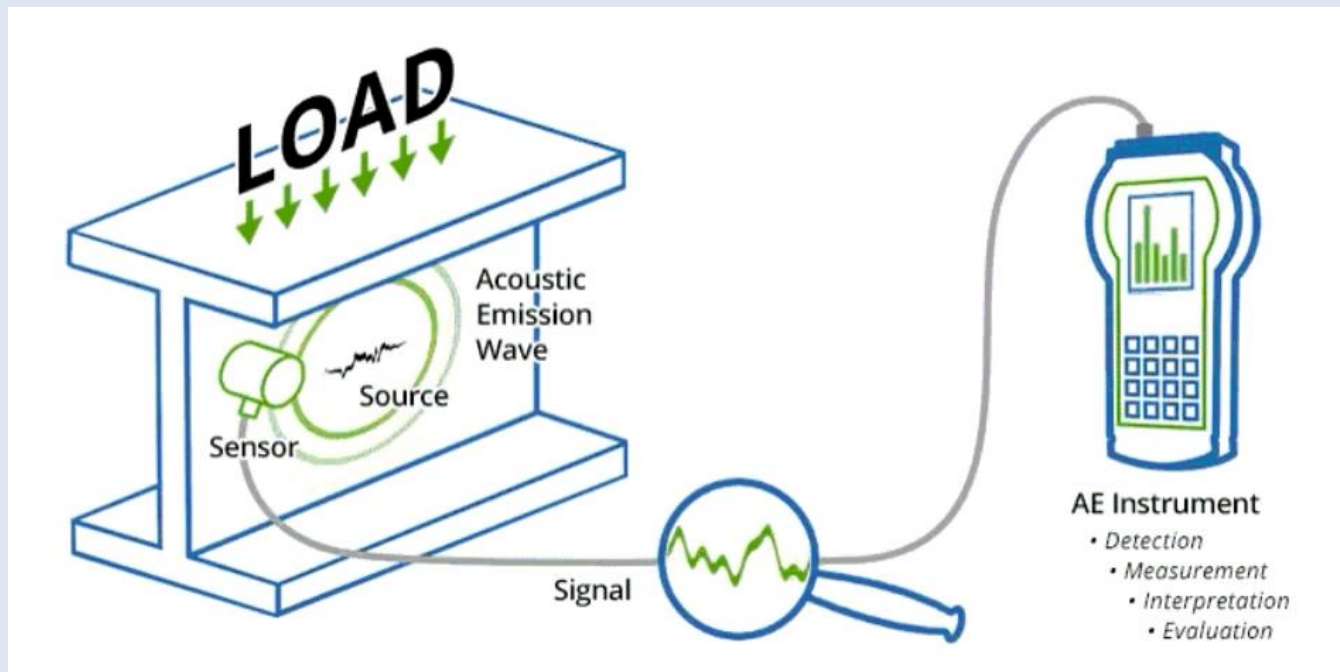






Can q-statistics interpret the AE in order to give information on the break-down point?

Acoustic emissions are caused by the rapid release of localized stress energy into the material for example as a result of **crack formation**. These elastic waves are recorded by means of sensors applied on the surface of the structure and then analysed.



AE have become in the last decades a very helpful tool for **Structural health monitoring** in structural engineering and concerns the determination of the state of health of a structure by means of the detection of changes in its response with respect to the undamaged one.

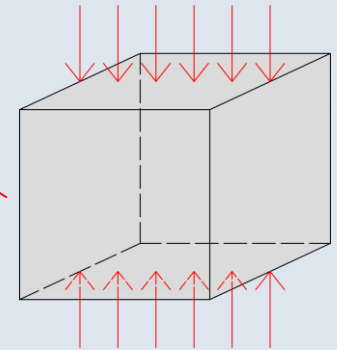
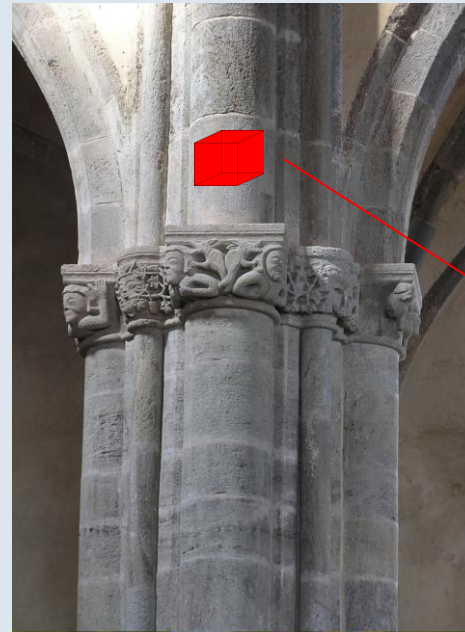
Small-scale damage is detectable long before failure, so AE can be used as a **non-destructive technique** for detecting hidden defects and evaluating material mechanical performance.



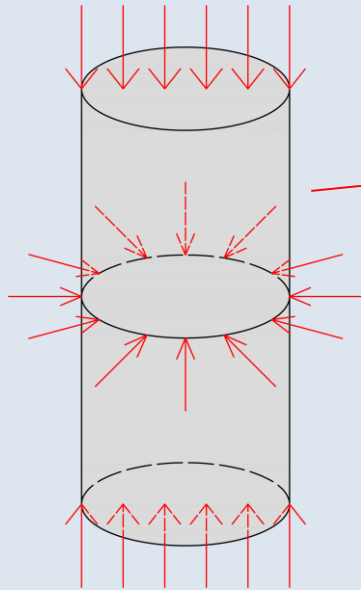
In this study we present the result of experimental tests performed on cubic specimens of **Concrete** and **Basalt** in the laboratory of the Department of Civil Engineering and Architecture of the University of Catania (Italy) and on cylindrical specimens of **Darley Dale Sandstone** and **Alzo Granite** performed in the Rock Mechanics Laboratory of the University of Portsmouth (United Kingdom)

In this study we present the result of experimental tests performed on cubic specimens of **Concrete** and **Basalt** in the laboratory of the Department of Civil Engineering and Architecture of the University of Catania (Italy) and on cylindrical specimens of **Darley Dale Sandstone** and **Alzo Granite** performed in the Rock Mechanics Laboratory of the University of Portsmouth (United Kingdom)

The cubic specimens have been tested under uniaxial compression load



In this study we present the result of experimental tests performed on cubic specimens of **Concrete** and **Basalt** in the laboratory of the Department of Civil Engineering and Architecture of the University of Catania (Italy) and on cylindrical specimens of **Darley Dale Sandstone** and **Alzo Granite** performed in the Rock Mechanics Laboratory of the University of Portsmouth (United Kingdom)



The cylindrical specimens have been tested under triaxial compression load in order to evaluate the effect of the confining pressure

Results from uniaxial cyclic compression tests on cubic specimens of Concrete and Basalt

Eur. Phys. J. Special Topics **229**, 841–849 (2020)
© EDP Sciences, Springer-Verlag GmbH Germany,
part of Springer Nature, 2020
<https://doi.org/10.1140/epjst/e2020-800232-7>

**THE EUROPEAN
PHYSICAL JOURNAL
SPECIAL TOPICS**

Regular Article

Acoustic emissions in compression of building materials: q -statistics enables the anticipation of the breakdown point

Annalisa Greco¹, Constantino Tsallis^{2,3,4}, Andrea Rapisarda^{4,5,6},
Alessandro Pluchino^{5,6,a}, Gabriele Fichera¹, and Loredana Contrafatto¹

Cubic specimens of concrete and basalt (150 mm side)



Concrete

Concrete is an **artificial conglomerate** consisting of a mixture of binder (cement), water and fine and coarse aggregates (sand and gravel)

Cubic specimens of concrete and basalt (150 mm side)



Basalt

Basalt is an effusive rock of volcanic origin, resulting from the escape of magma. The basalt samples tested in this study came from the quarries on the **ETNA** volcano.

Cubic specimens of concrete and basalt (150 mm side)

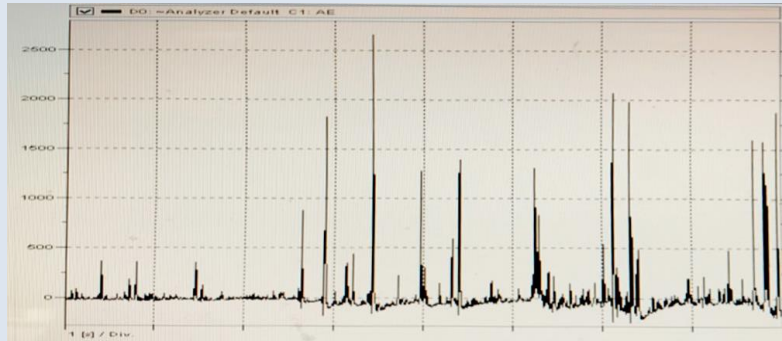


Concrete

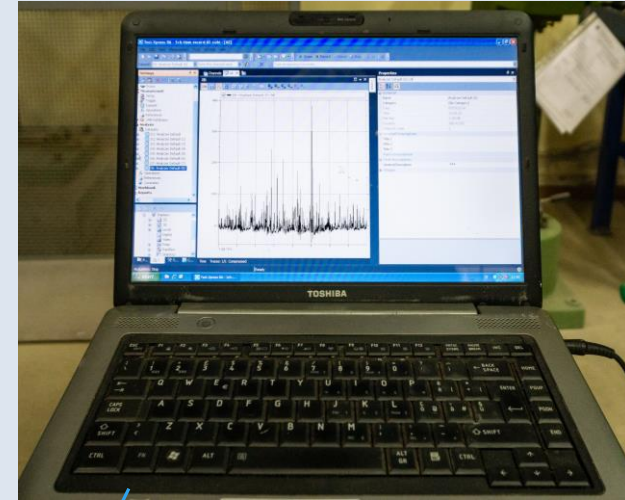
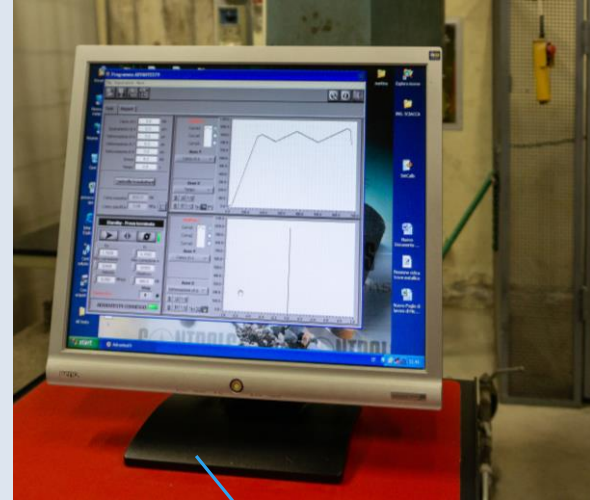
Basalt

The acoustic emission (AE) produced by the growth of local micro-cracks associated with the fracture phenomenon during cyclic compression have been recorded and analyzed.

Acoustic emissions during the tests were measured through a sensor capable to measure emissions of surface and longitudinal waves over a broad high frequency range, 50-400 KHz



The analogic output signal was recorded by a data acquisition front end and successively post processed.

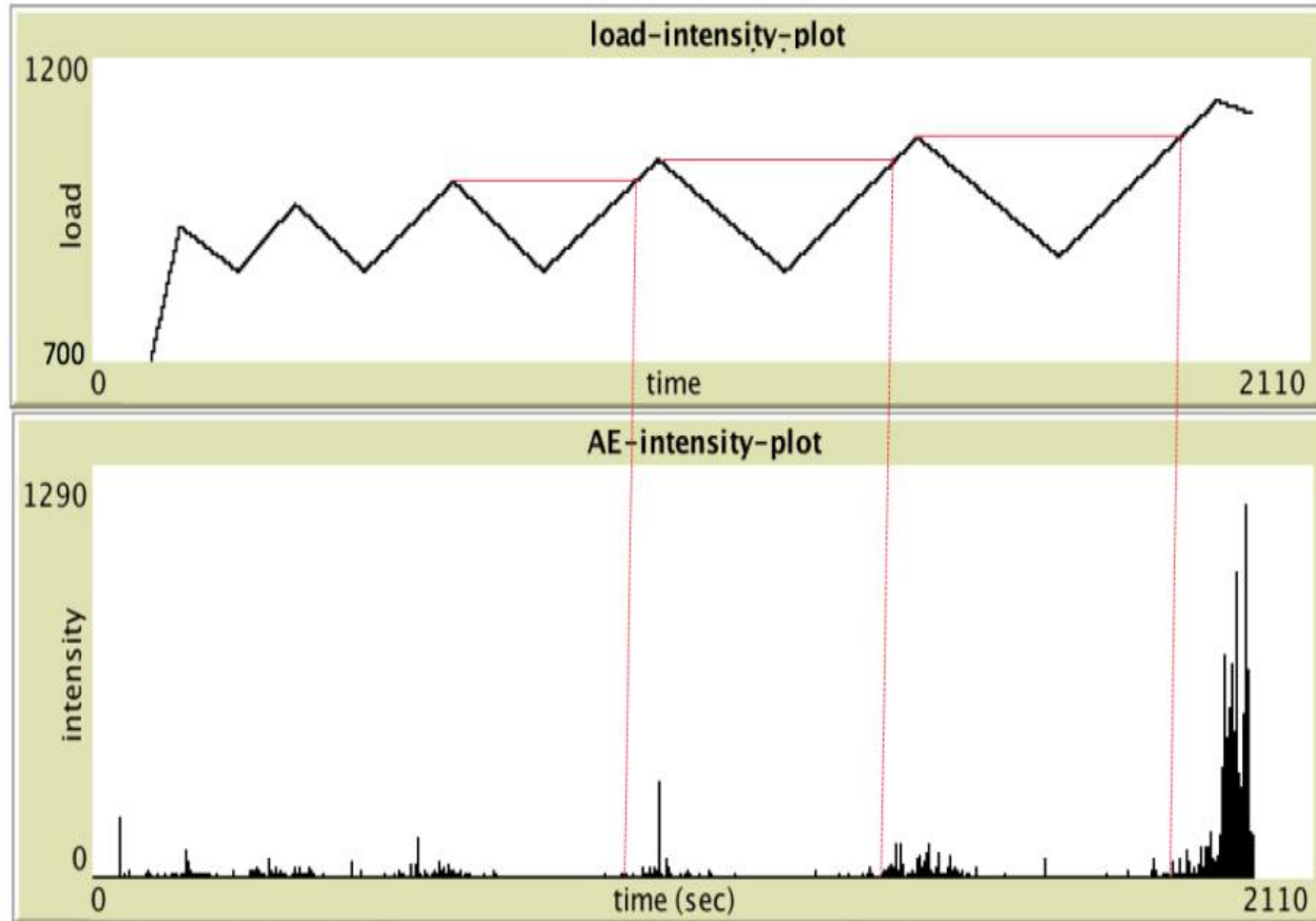


The cyclic compression tests, with load control, have been performed on several cubic specimens of both the chosen materials using a 5000 KN hydraulic press connected to a data acquisition unit.

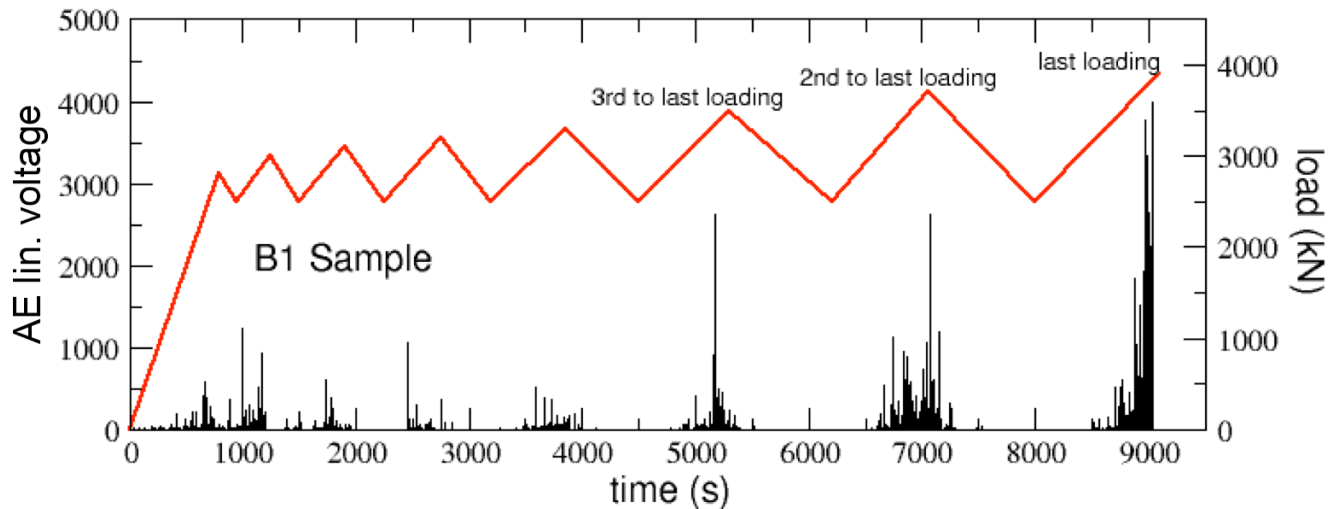
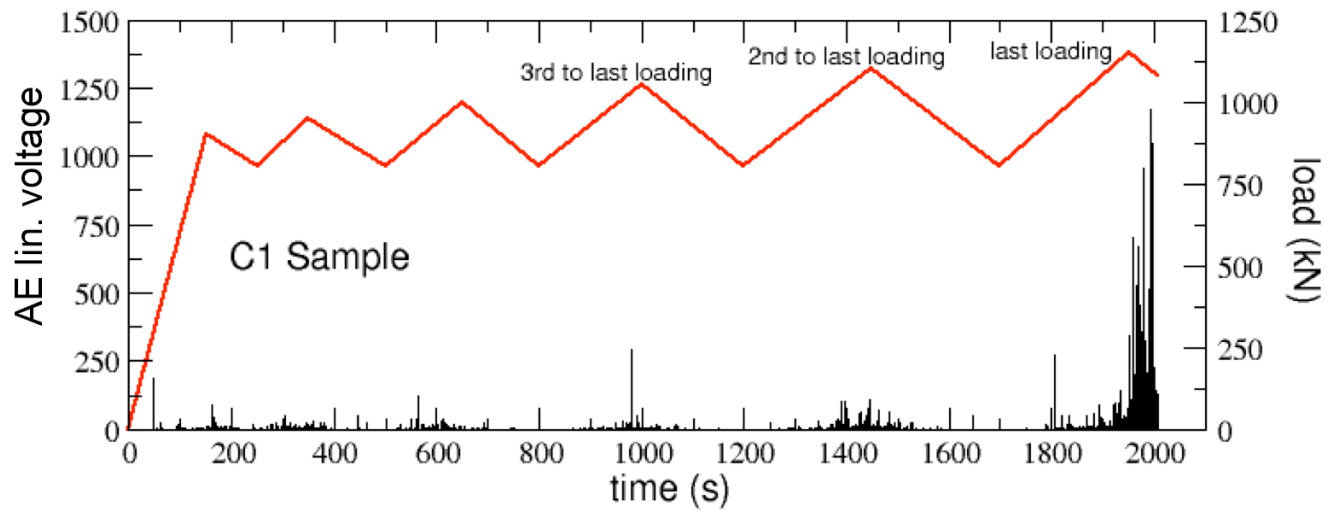
Material	Load step (kN)	Average Failure load
Concrete	0 -> 900 -> 800 -> 950 -> 800 -> 1000 -> 800 -> 1050 -> 800 -> 1100 -> 800 -> 1150 -> 800 -> 1200	1154
Basalt	0 -> 2800 -> 2500 -> 3000 -> 2500 -> 3100 -> 2500 -> 3200 -> 2500 -> 3300 -> 2500 -> 3500 -> 2500 -> 3700 -> 2500 -> 3900 -> 2500 -> 4000	3829

In each loading and unloading step (except for the first loading starting from zero, which is faster), a progressive increment rate of 0.05 MPa/s has been selected

KAISER EFFECT



The micro-cracks opened in the material during the loading phases do not propagate until a load intensity greater than the one previously experienced is reached



For **concrete specimens**, the acoustic emissions started from high values of the applied load and were concentrated at the load peaks.

In **basalt specimens**, high intensity emissions started immediately after the application of the first loading and lasted throughout the tests

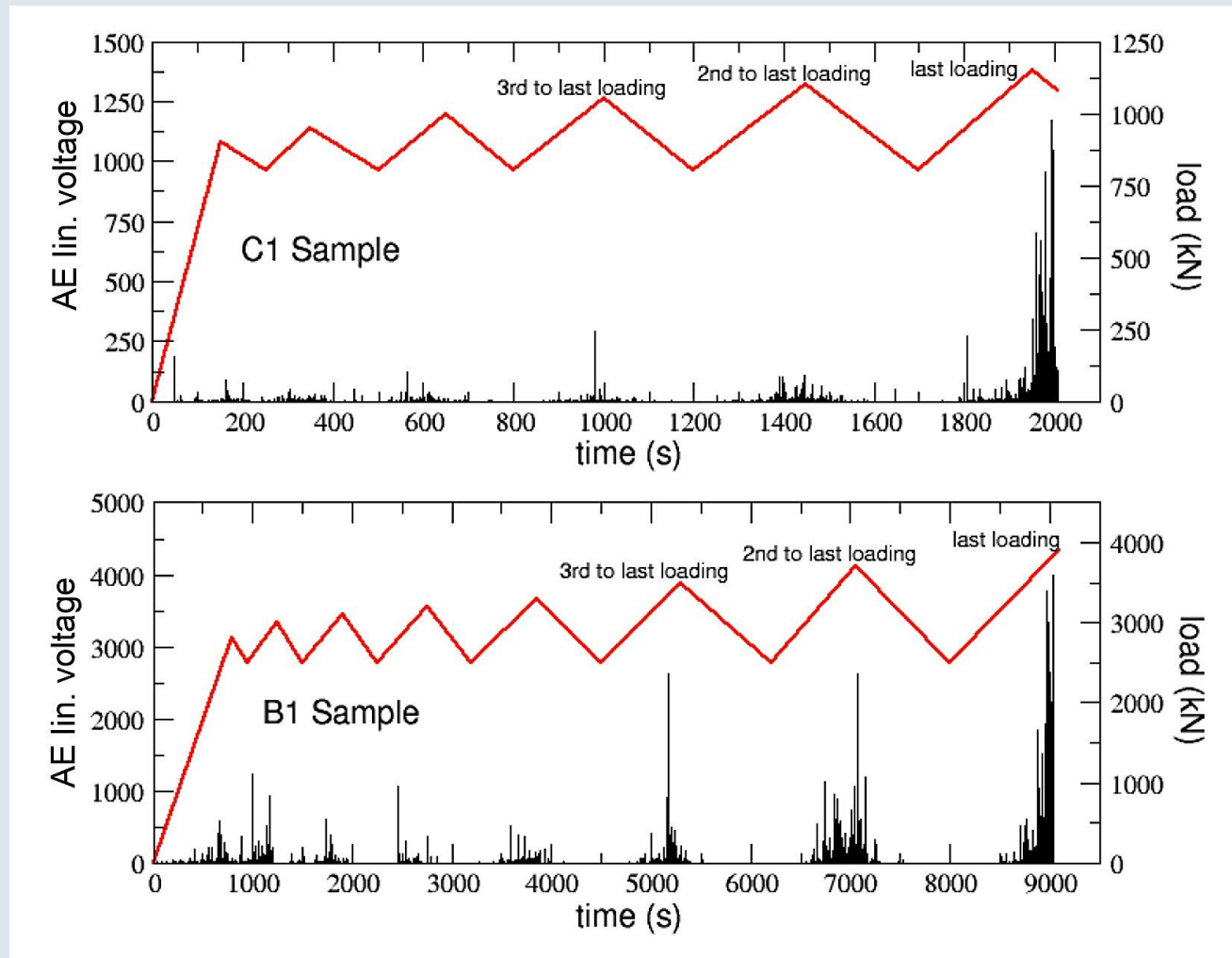


The failures for the considered samples occurred:

after 2007 seconds at a load value of 1080KN for the concrete sample C1

after 9101seconds at a load value of 3902KN for the basalt sample B1

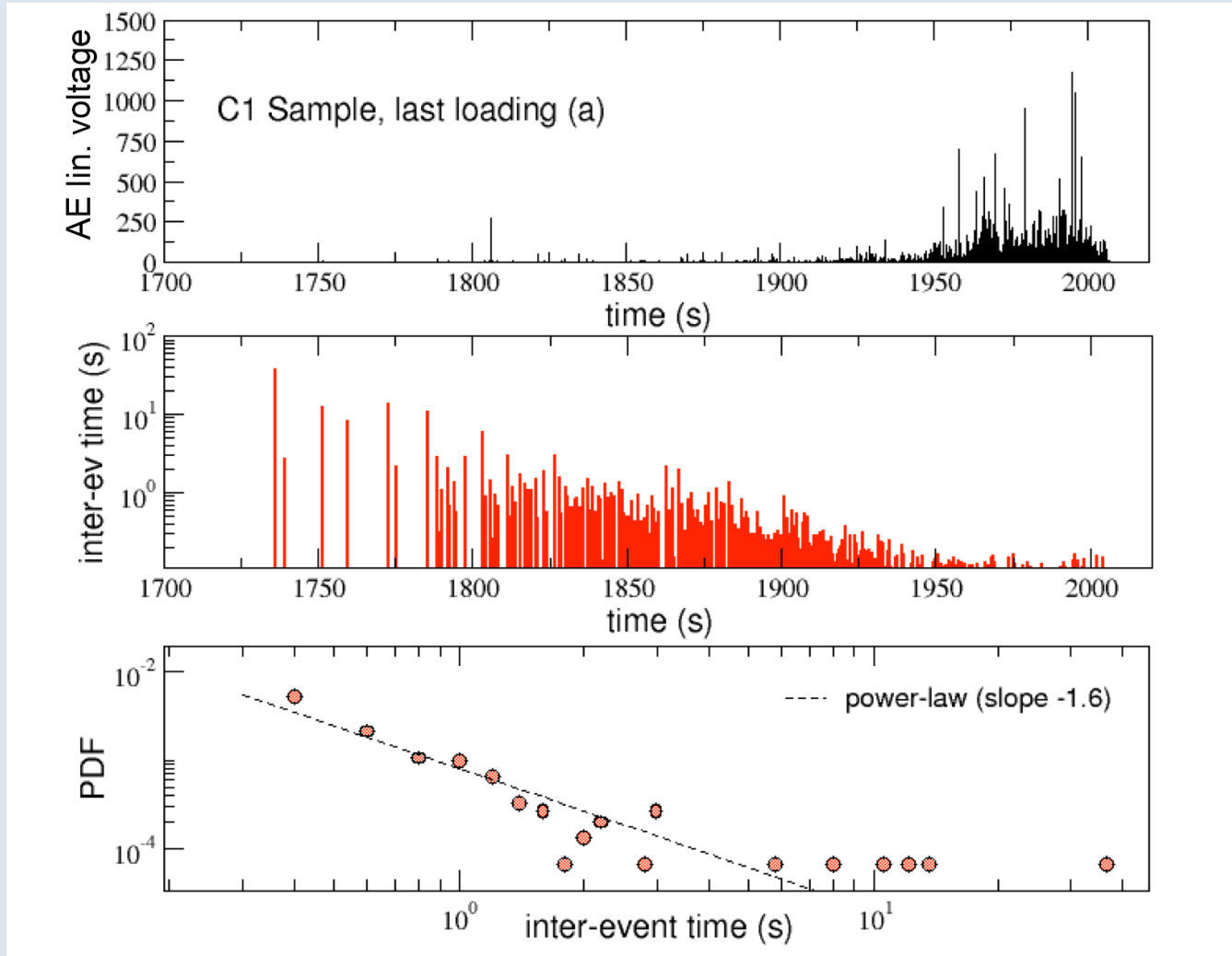
Let us investigate, now, the inter-event time series of the AE recordings during the compression tests on some of the considered specimens



The inter-event time $\delta\tau(t)$ is defined as the time interval between two consecutive recordings $AE(n)$ and $AE(n-1)$:

$$\delta\tau(t) = t_{AE(n)} - t_{AE(n-1)}$$

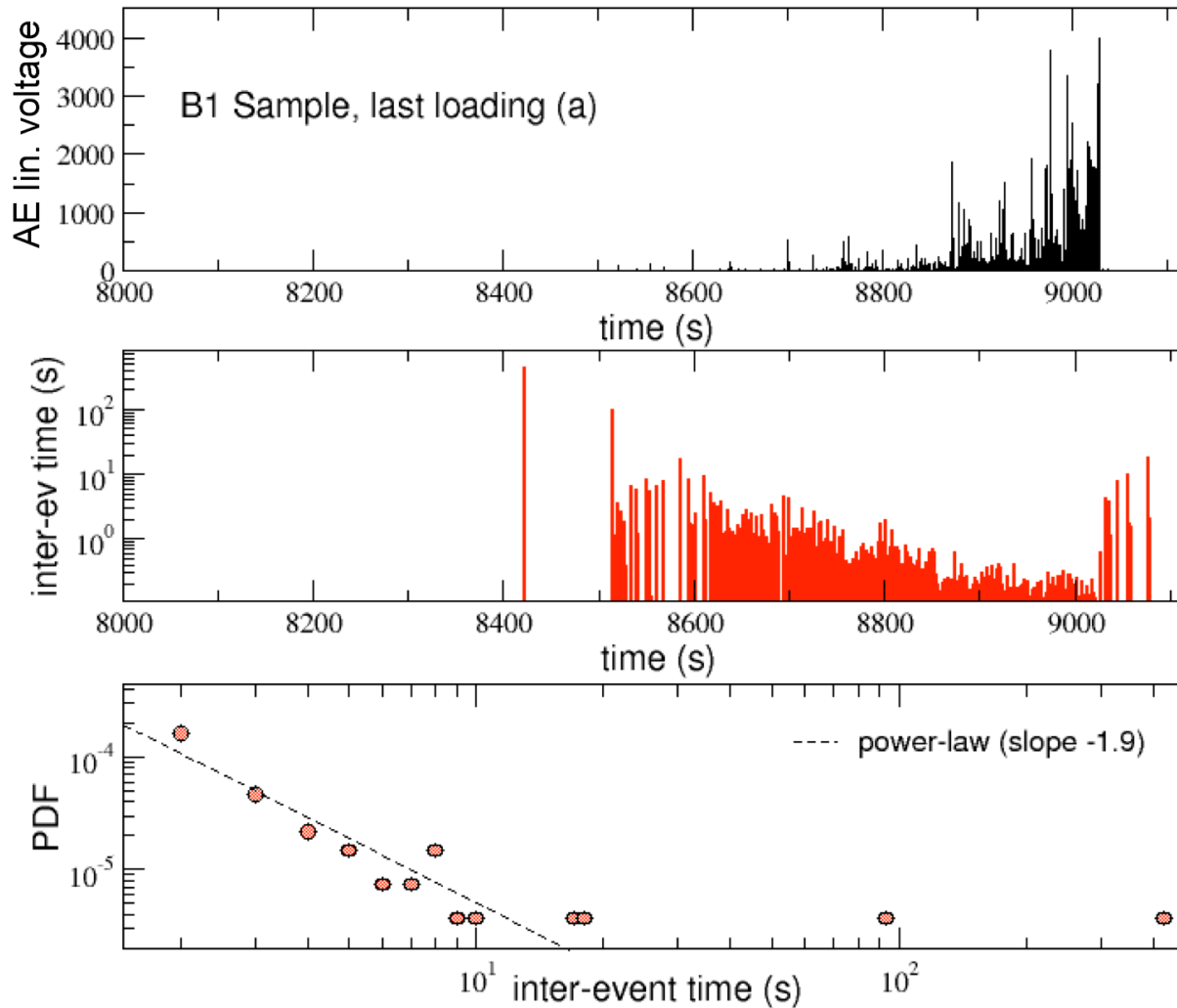
From top to bottom: the AE recordings of the last loading, the corresponding inter-event time series $\delta\tau(t)$ and the probability distribution function $P(\delta\tau)$



COMPRESSION
TEST ON
CONCRETE SPECIMEN

The $P(\delta\tau)$ distribution can be well fitted (in log-log scale) by power-law curves thus highlighting the **complex behavior** of the failure process

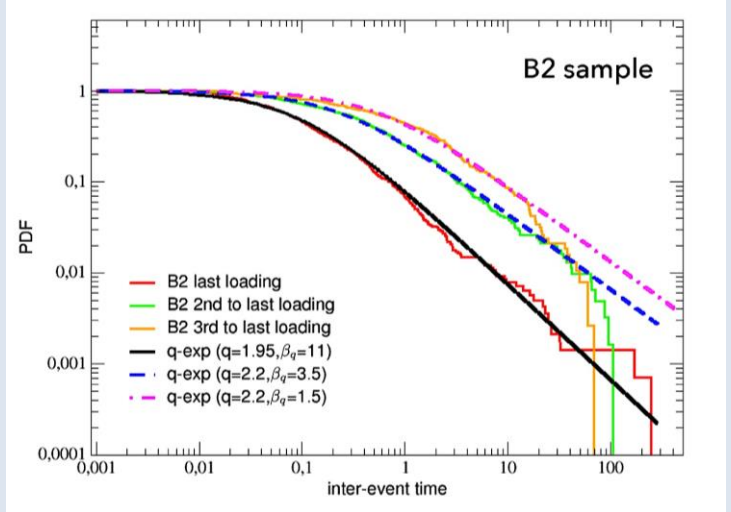
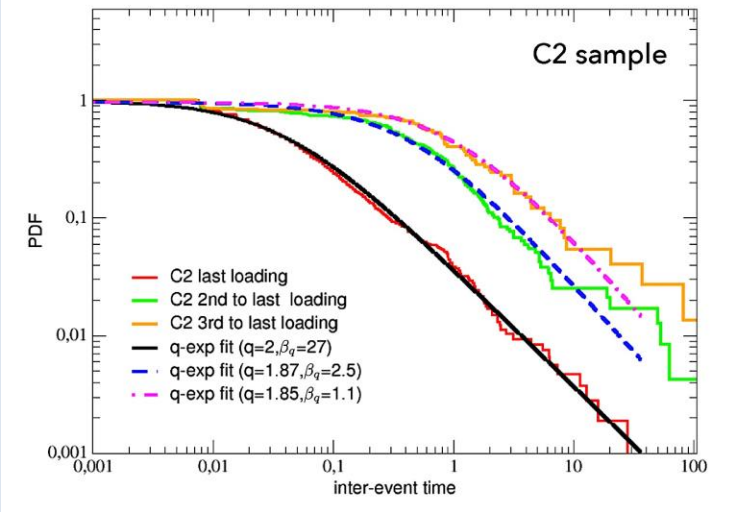
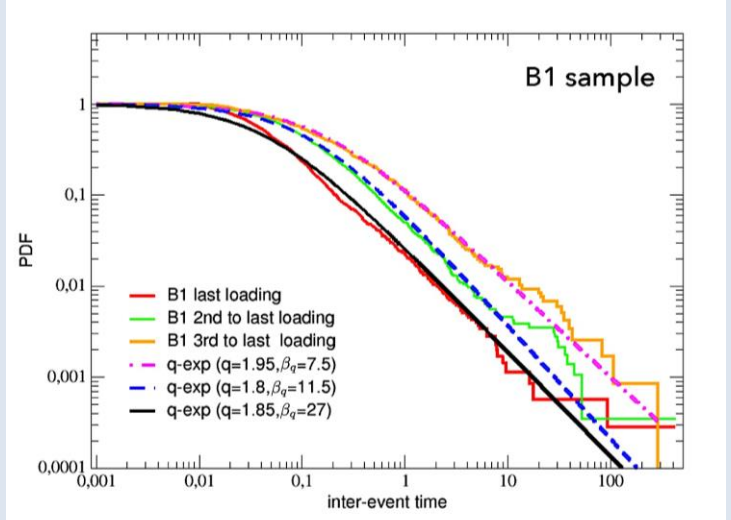
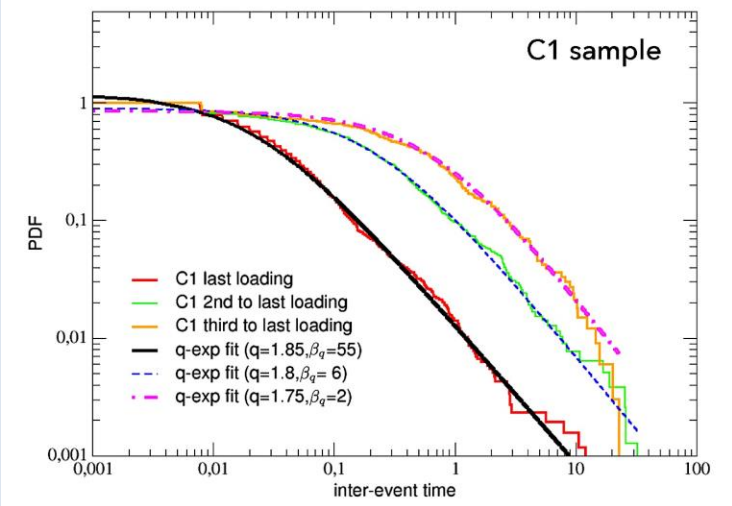
From top to bottom: the AE recordings of the last loading, the corresponding inter-event time series $\delta\tau(t)$ and the probability distribution function $P(\delta\tau)$



COMPRESSION TEST
ON **BASALT SPECIMEN**

Greater value of the slope of the power law fitting curve

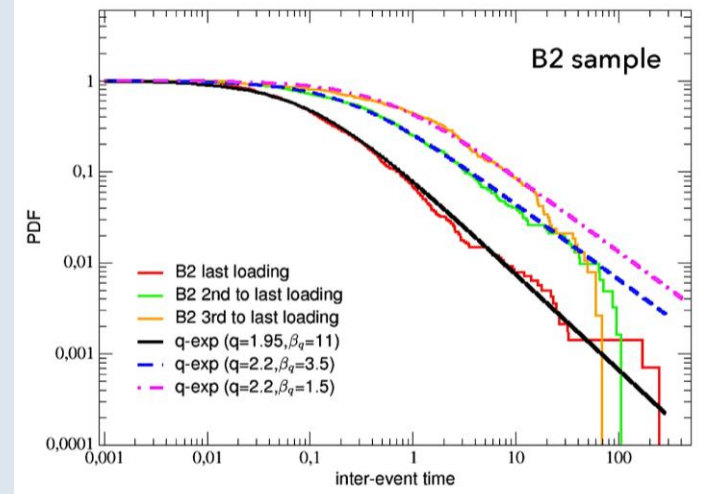
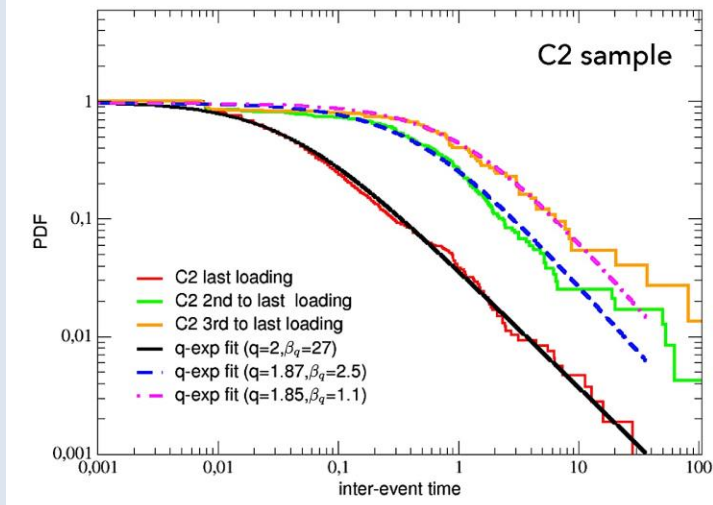
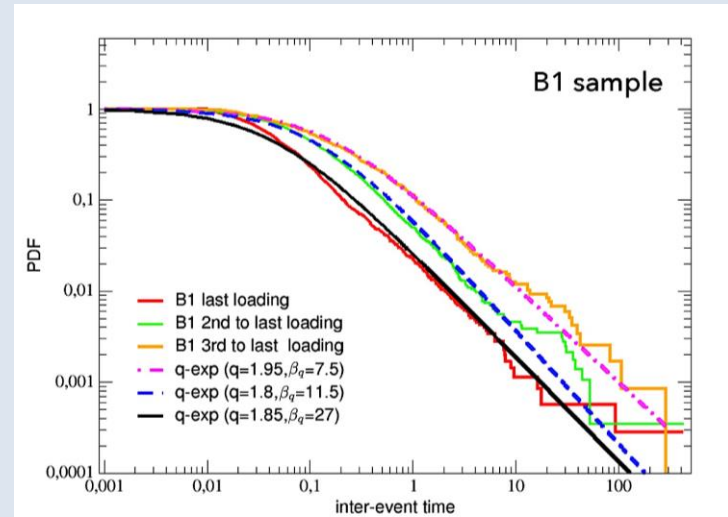
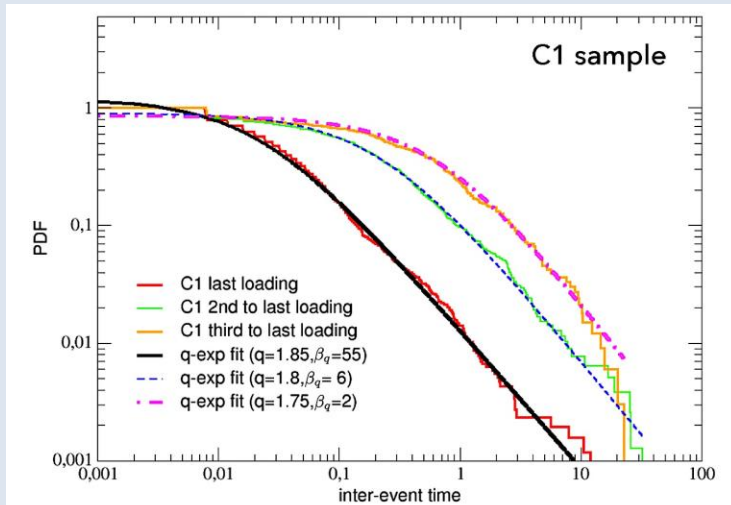
The complex behavior of the inter-event time series will be analyzed in terms of **complementary cumulative distribution functions $P(> \delta\tau)$** which reports, for each value of $\delta\tau$, the fraction of inter-event times greater than that value.



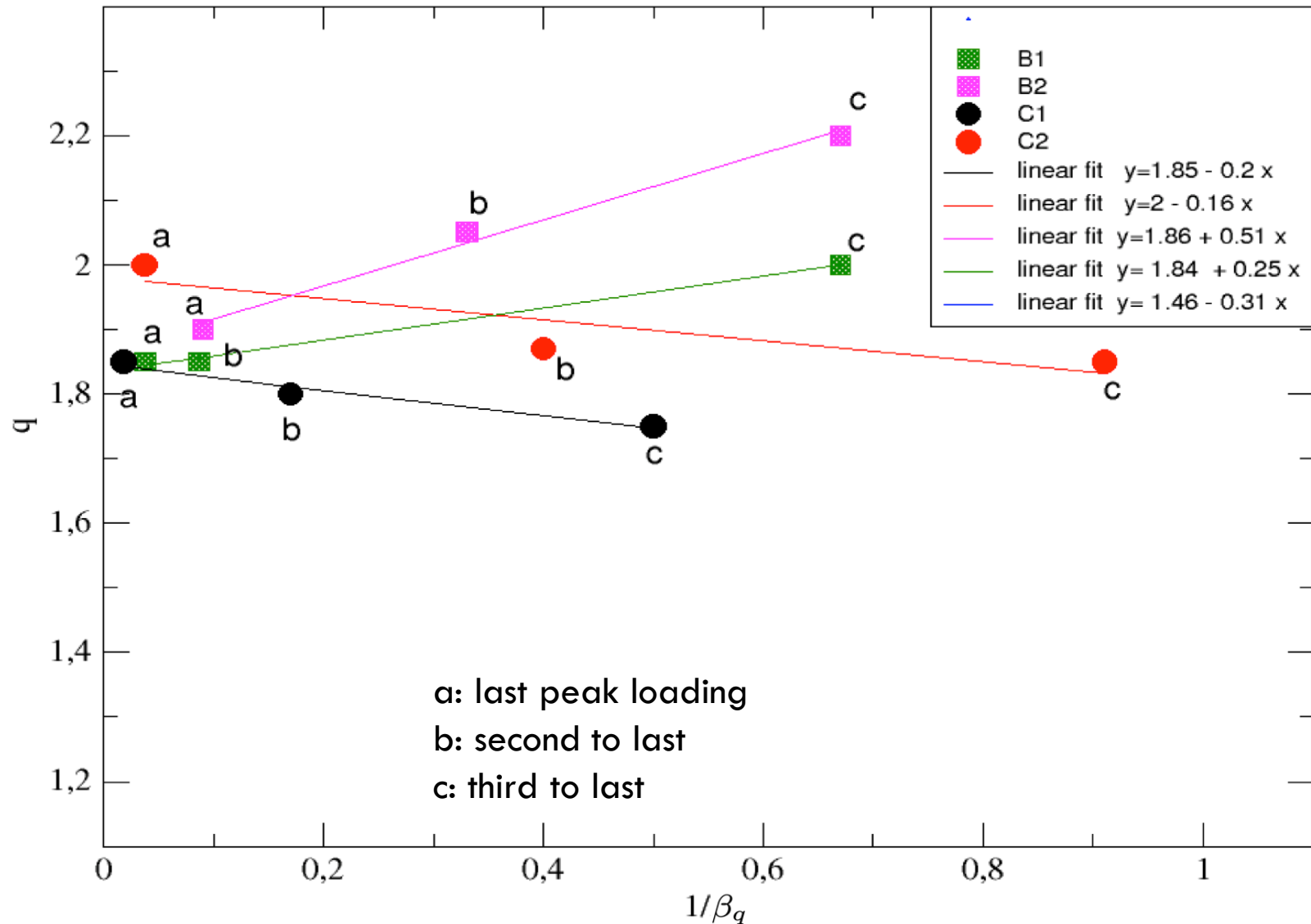
As expected, all the reported data show **a power-law tail after an initial saturation**

This behavior can be very well reproduced by means of a decreasing q-exponential function:

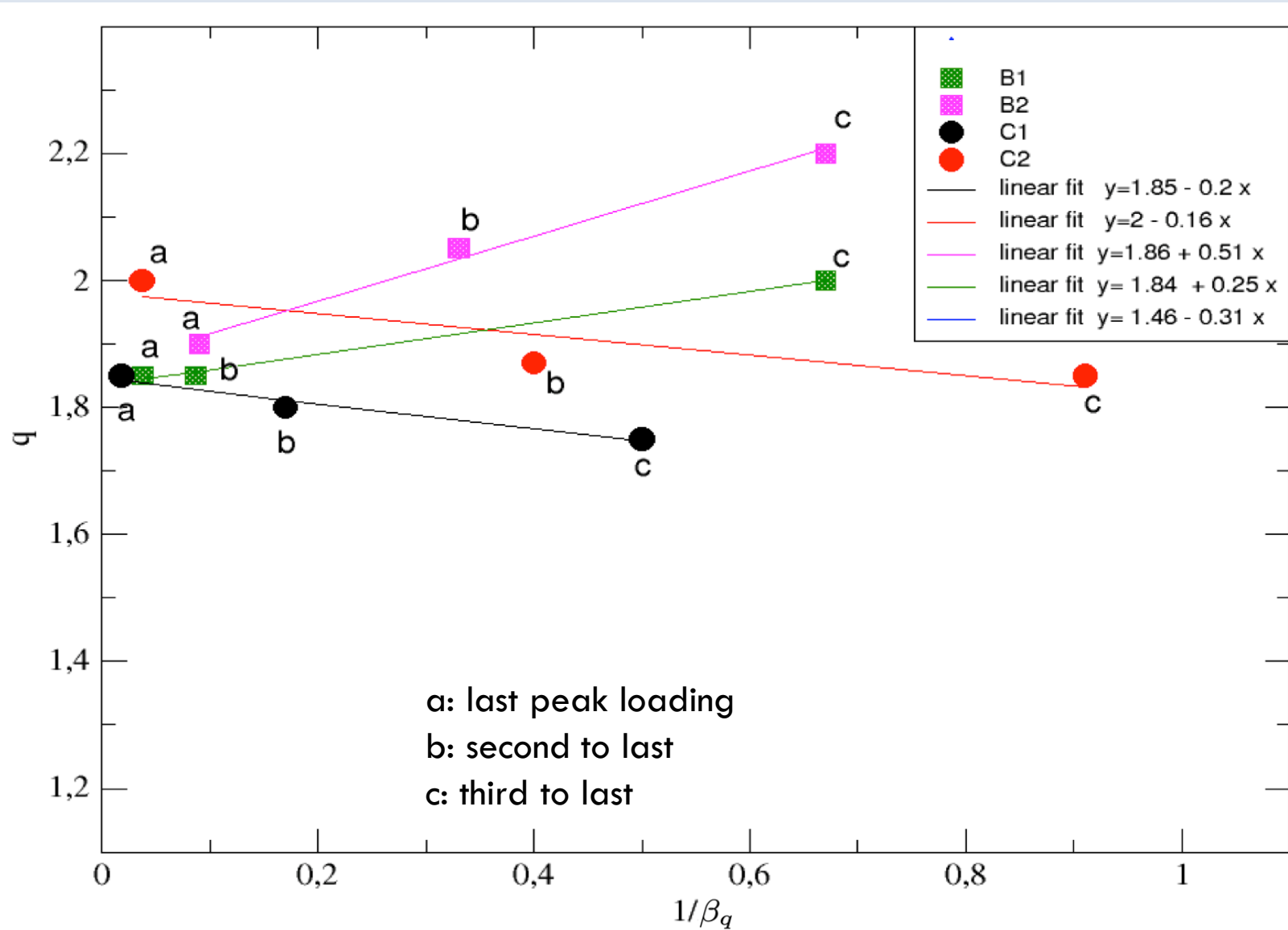
$$e_q(\delta\tau) = [1 - (1 - q)\beta_q\delta\tau]^{1/(1-q)}$$



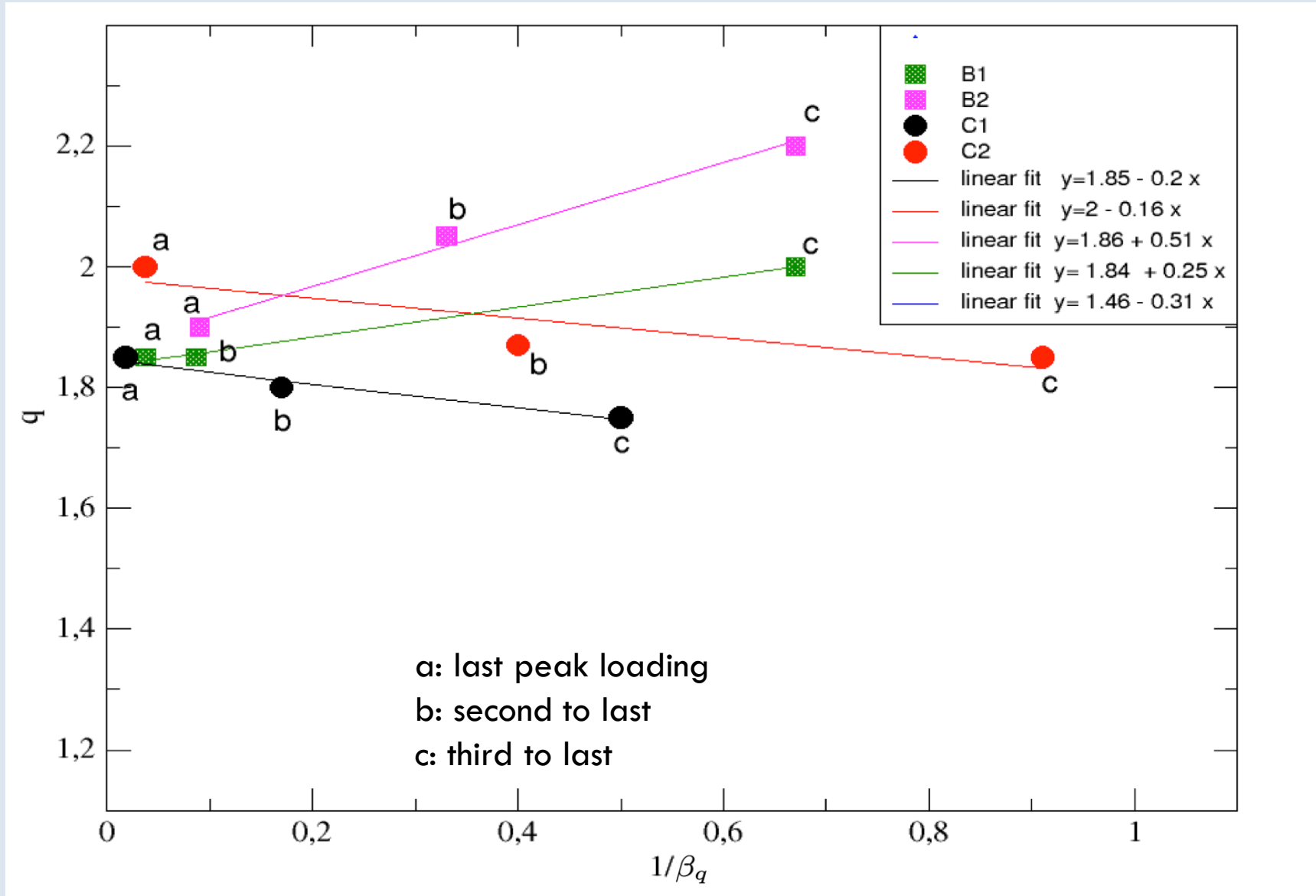
In this context we look for the existence of a **relationship between the entropic index q and $1/\beta_q$** (level of noise) able to characterize the behavior of the materials in the proximity of the failure:



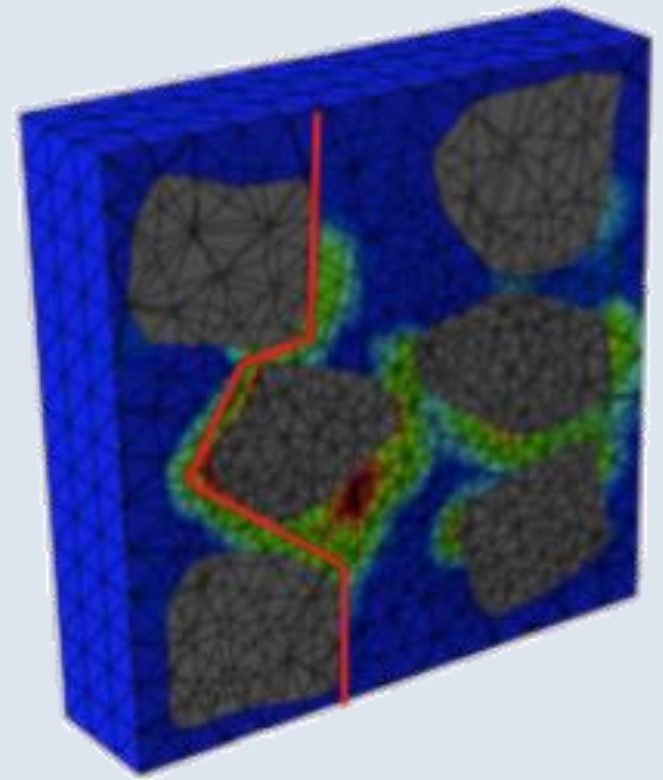
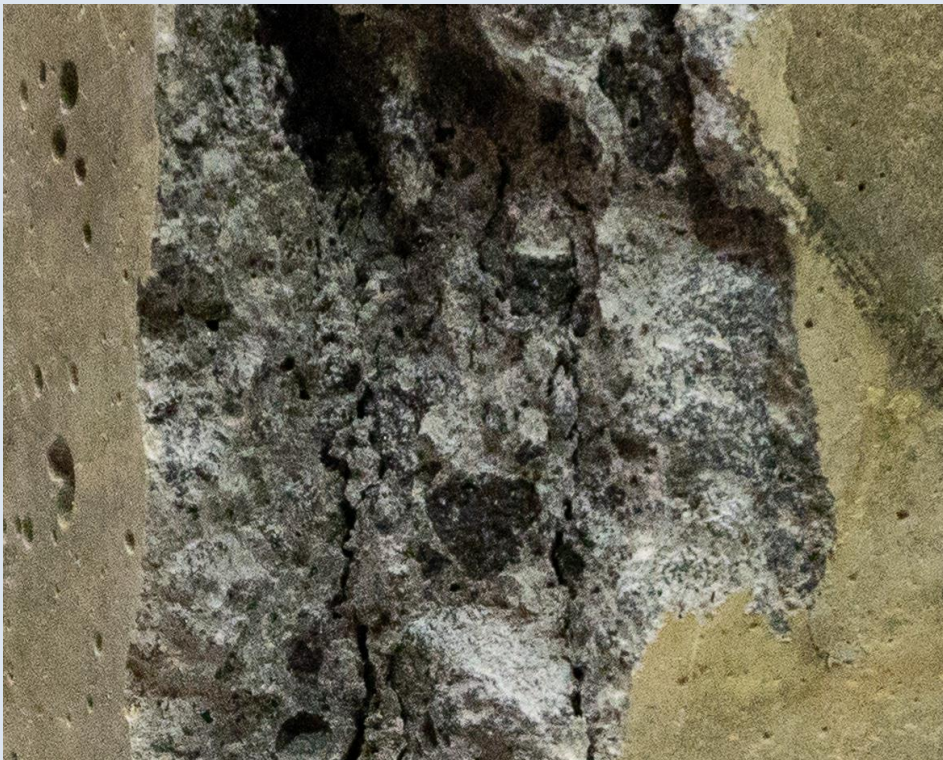
Approaching the failure, while $1/\beta_q$ tends to zero, the entropic index q goes towards a value in between 1.8 and 2.0.



Approaching the failure point the trend is increasing for the concrete specimens and decreasing for the basalt ones. This fact reflects the different behavior of the two materials while they go towards the rupture.



Being a **composed material** concrete breaks very slowly when increasing the compression, with fractures propagating along preferential lines which, as can be observed at a mesoscopic scale, **surround the aggregates**. This phenomenon could be responsible of the **long-range correlations** quantified by increasing values of q .

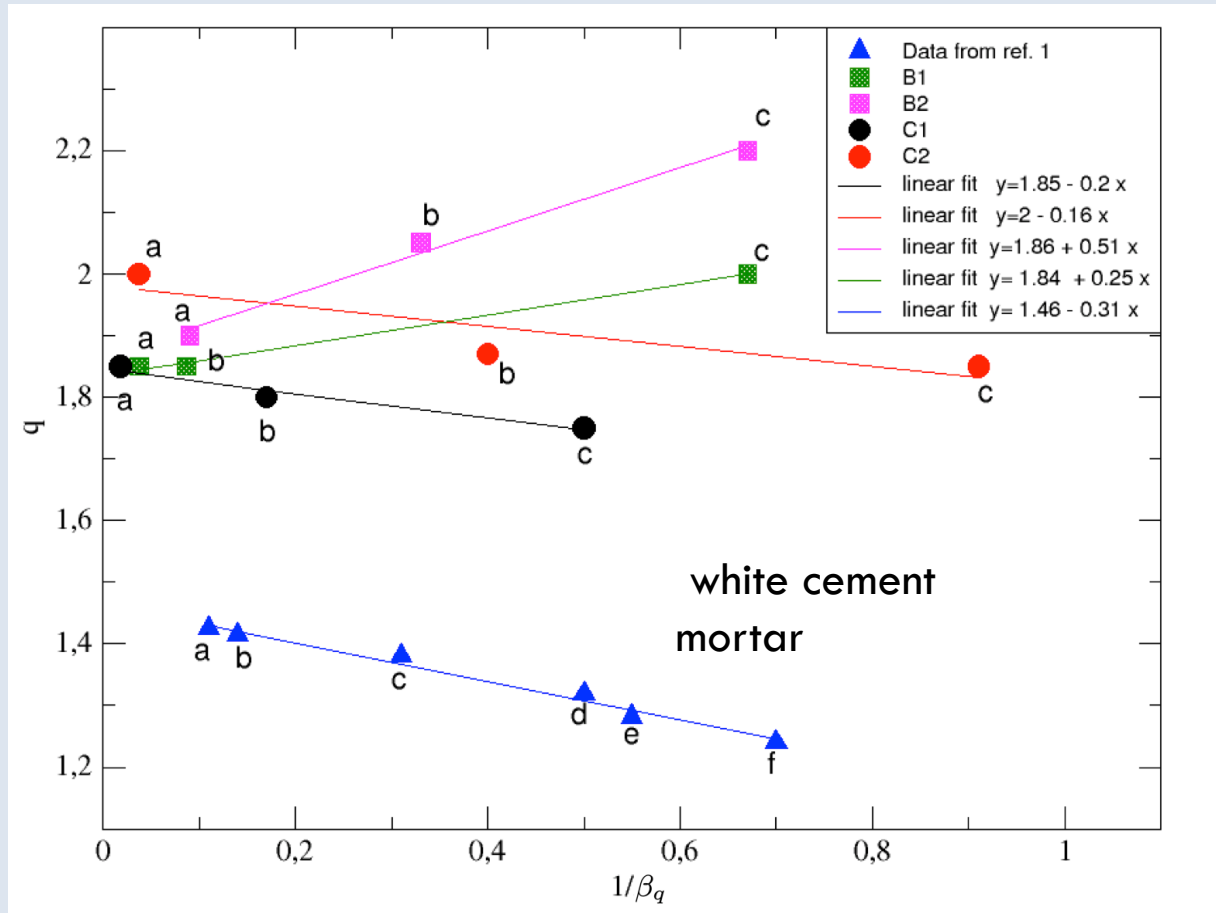


On the contrary, being a more compact and homogeneous natural material **basalt** tends to **uniformly resist to stronger compressions** until it suddenly breaks in a kind of explosive way: the value of q decreases approaching $1/\beta_q = 0$.




It is interesting to compare these results with those reported in the paper:

I. Stavrakas, D. Triantis, S.K. Kourkoulis, E.D. Pasiou, I. Dakanali, Latin Am. Journ. of Sol. and Struc. 13 (2016) 2283



Both **concrete and cement mortar**, although at different scales, are composed by a **mixture of binder and aggregates** which can drive the propagation of cracks along the preferential directions surrounding the aggregates

Results from tri-axial compression tests on cylindrical specimens of Darley Dale Sandstone and Alzo Granite



Submit to this Journal

Review for this Journal










Propose a Special Issue







IK

Open Access Article

Order Article Reprints

Acoustic Emissions in Rock Deformation and Failure: New Insights from Q-Statistical Analysis

by  Sergio C. Vinciguerra ¹  ,  Annalisa Greco ²  ,  Alessandro Pluchino ^{3,4}  ,

 Andrea Rapisarda ^{3,4,5}   and  Constantino Tsallis ^{5,6,7,*}  



Darley Dale Sandstone (DDS) porosity 14% is a medium to coarse grained, hard, granular sandstone which is well sorted with a rough feel. It comprises darker brown ferruginous specks, feldspar and occasional flecks of mica.



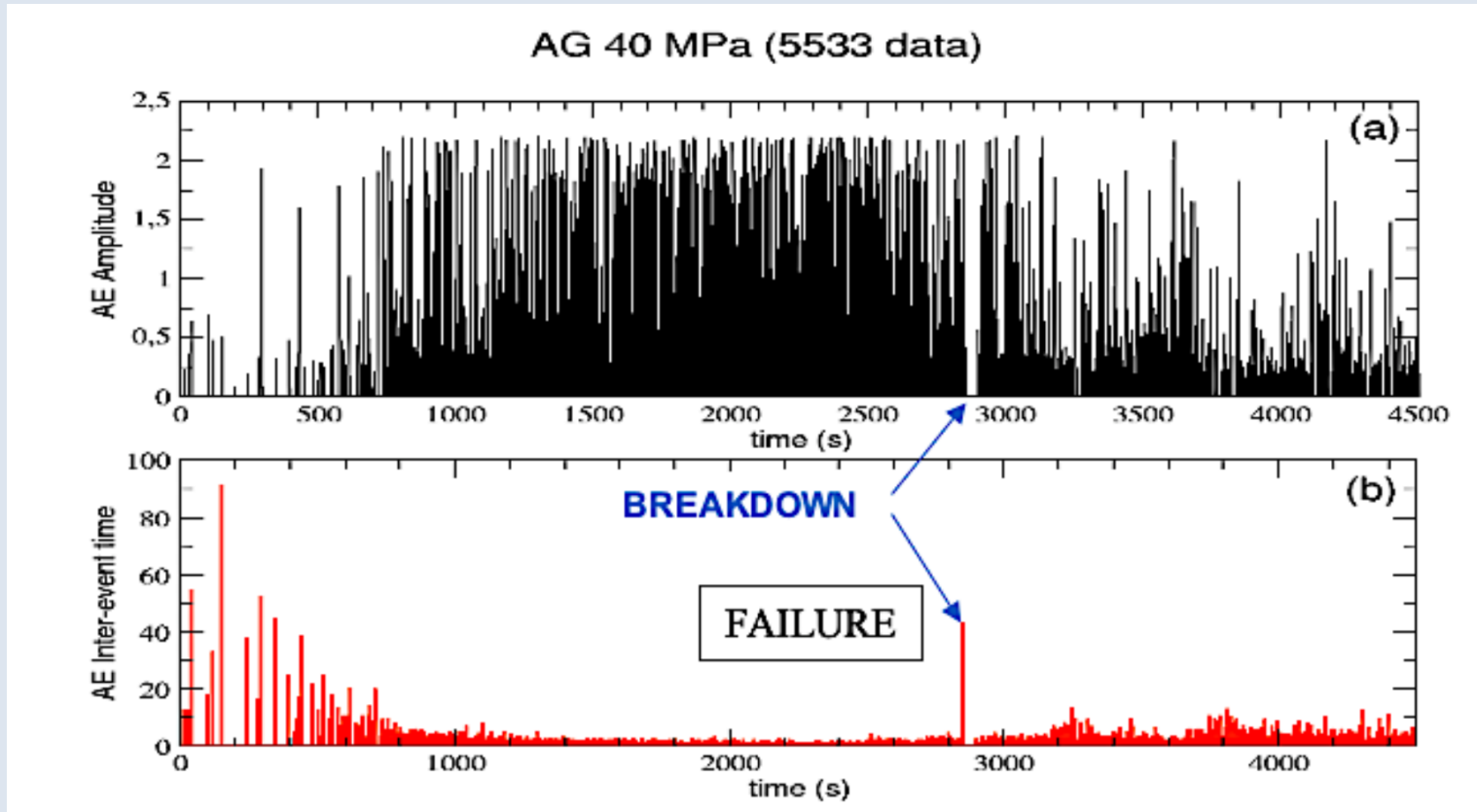
Alzo Granite (AG) porosity < 1% is an intrusive compact magmatic rock formed over 280 million years ago: the name of the **stone** comes from the Latin “granum”, that is, made in “grains”



TRIAXIAL TEST APPARATUS:
A) Control panel B) Triaxial cells

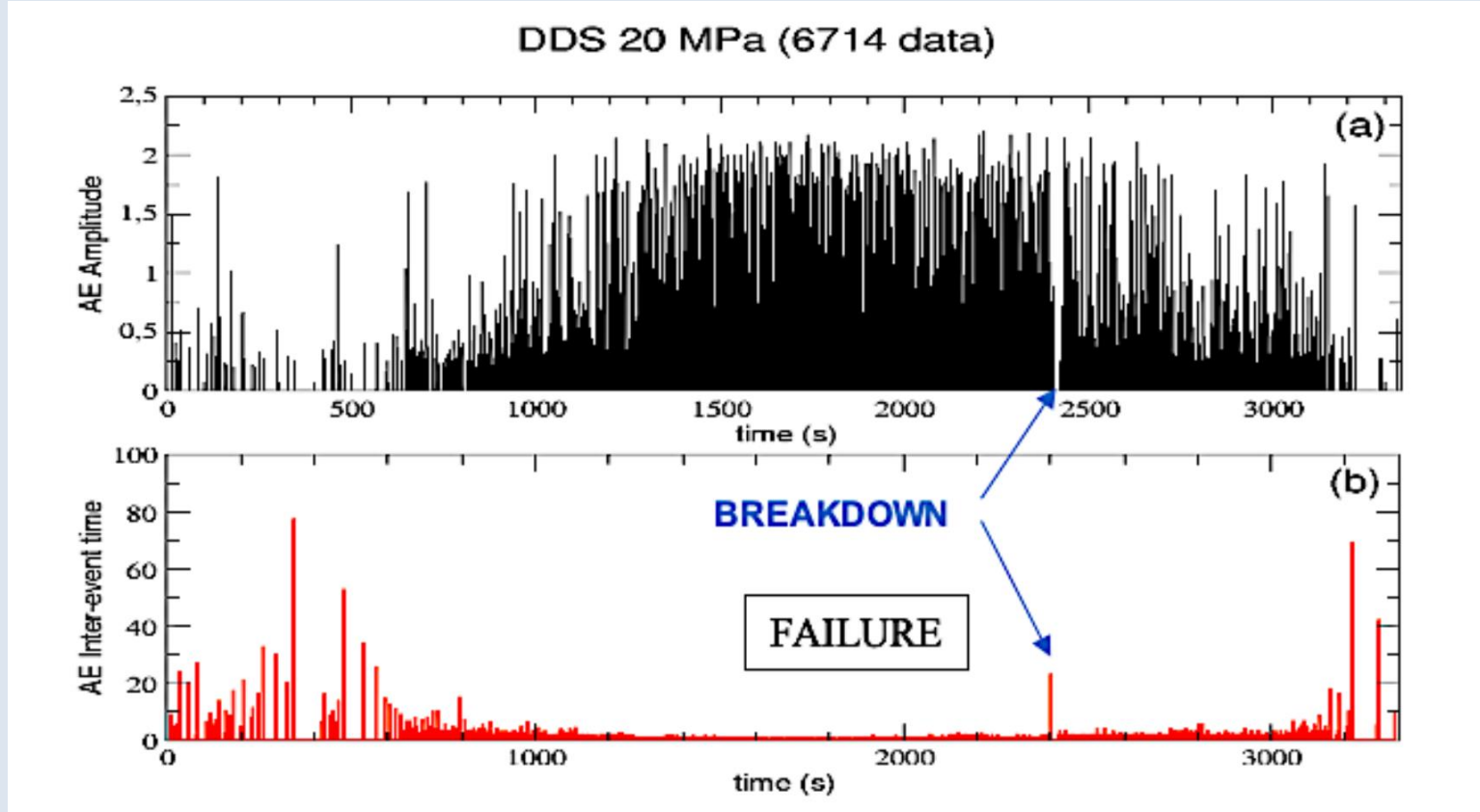
Cylindrical 40mm x 100mm samples with an array of twelve 1MHz single-component Piezo-Electric Transducers for AE detection (REF).
Triaxial compression tests have been performed at 5,10,20 and 40MPa

AE Amplitude (a) and inter-event time (b) as function of time (s)

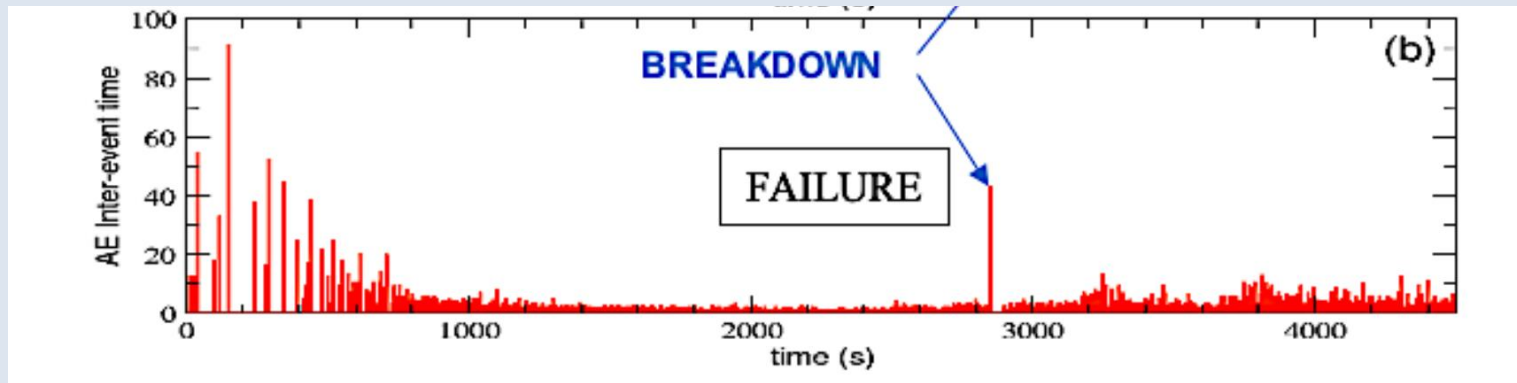


AG shows an **abrupt increase at the end of the elastic phase**, between 500 and 1000 seconds, then AE amplitude remains quite constant until failure (which happens at about 2800s) and, finally, it decreases during the post-failure phase.

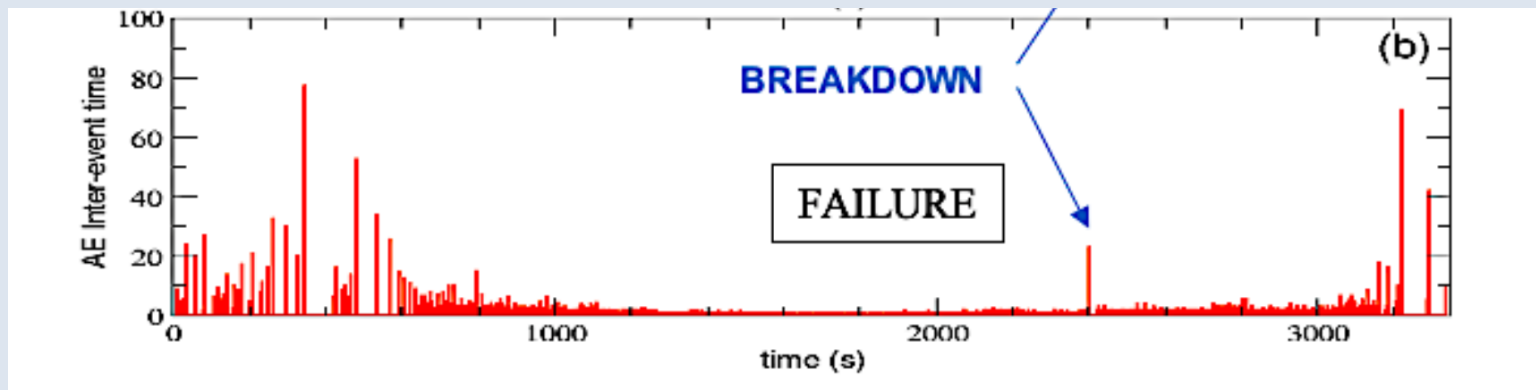
AE Amplitude (a) and inter-event time (b) as function of time (s)



DDS presents a much **more gradual AE amplitude increase** from 500 to 1500 seconds, reaching steady values before failure **therefore it shows a much clear premonitory phase**, or foreshock, before a critical damage threshold (which happens at about 2400s), then a decrease driven by the post-failure stick-slip processes.



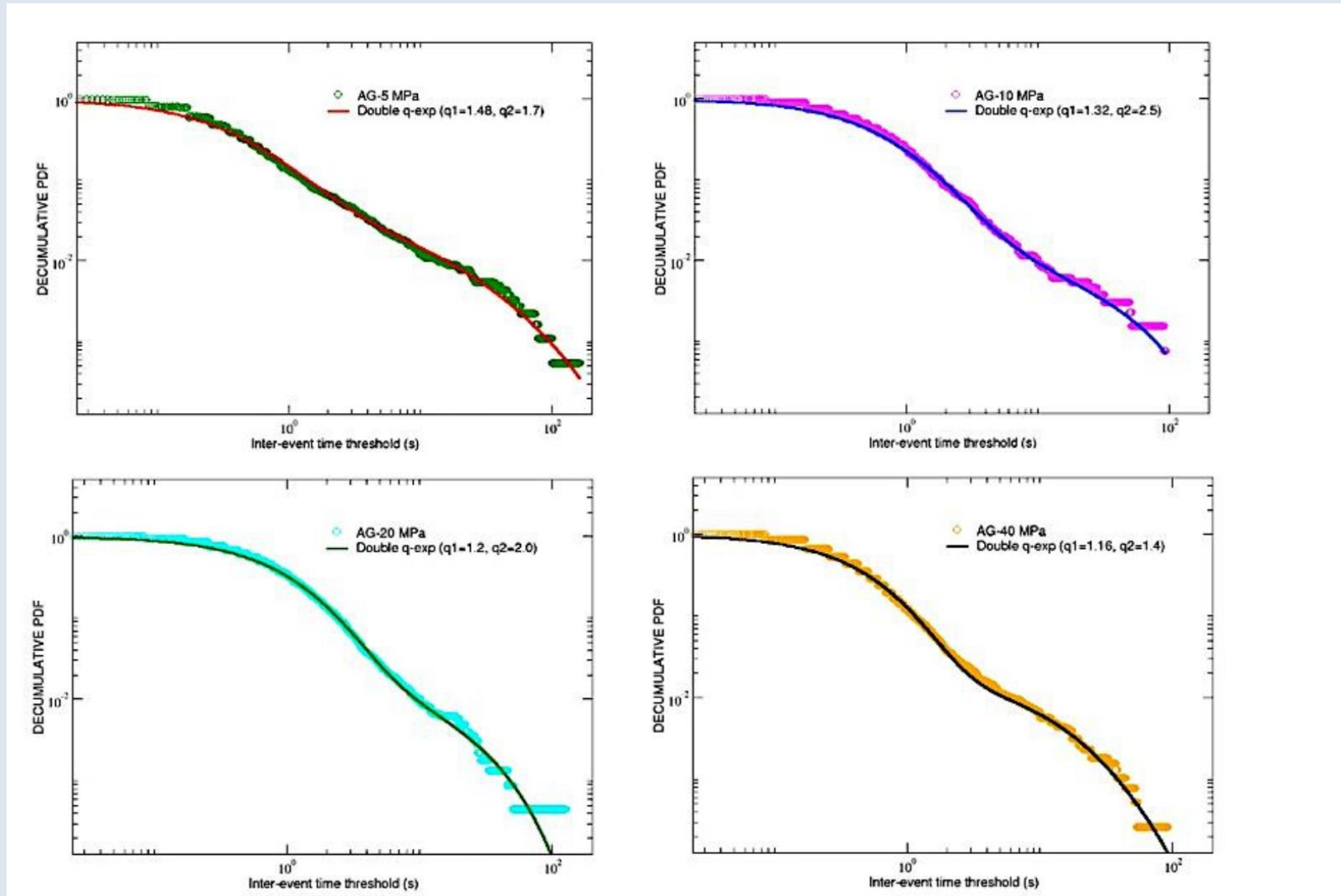
AG



DDS

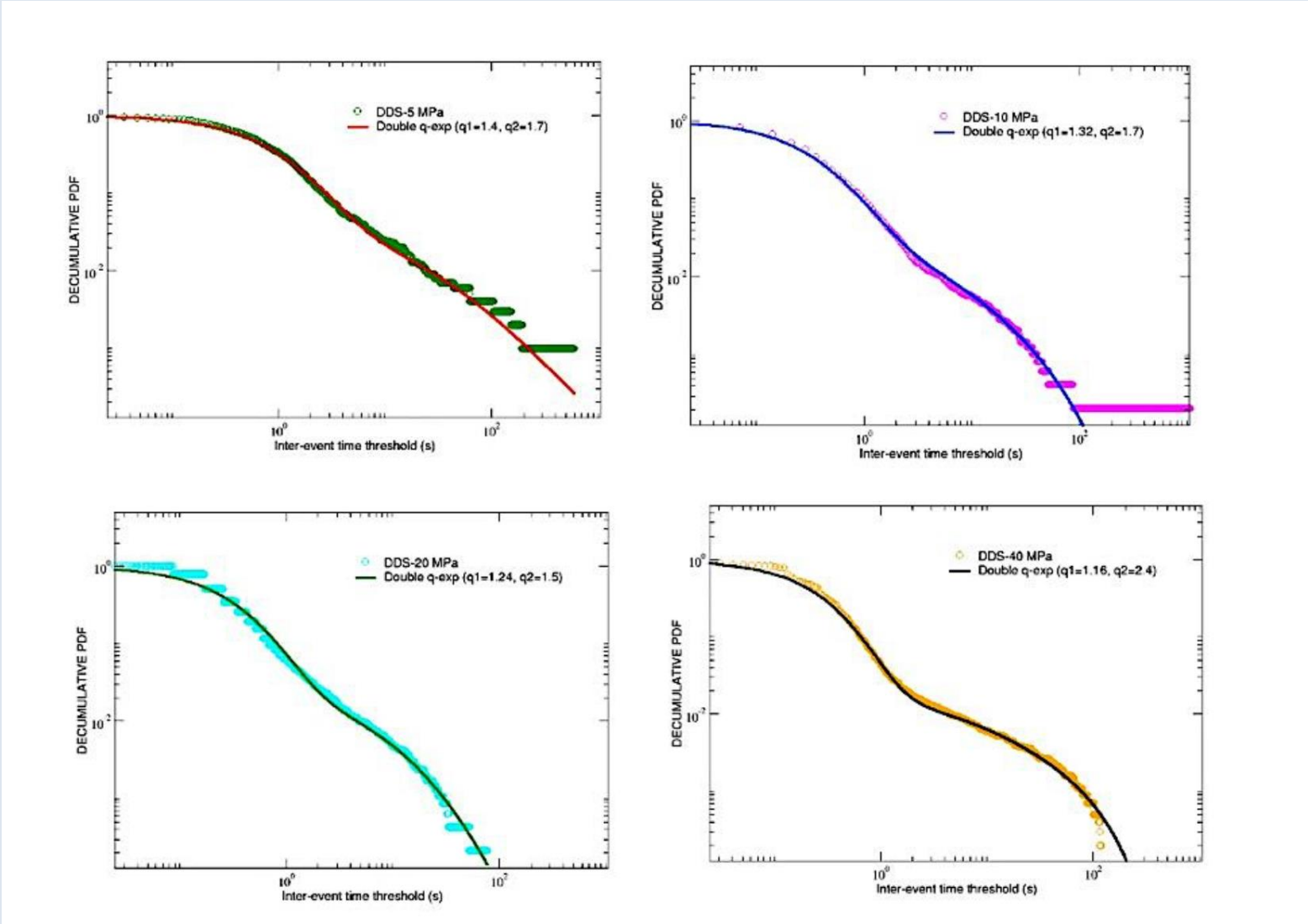
For both the samples, **failure is characterized by a peak in the AE interevent time**, which suddenly appears after a sequence of very low values corresponding to the sequence of high amplitude events before rupture.

Complementary cumulative (decumulative) probability distributions of AE inter-event times for the AG samples



The decumulative PDFs seem to further change slope in correspondence of a **second inflection point**

Complementary cumulative (decumulative) probability distributions of AE inter-event times for the DDS samples



The decumulative PDFs seem to further change slope in correspondence of a **second inflection point**

Complementary cumulative (decumulative) probability distributions of AE inter-event times for the AG and DDS samples.

This new kind of behavior **could be still described in the framework of q -statistics**, but adopting the following more general fitting function

$$y = A(1 - (1 - q_1)\beta_1 x)^{\frac{1}{1-q_1}} + (1 - A)\left(1 - \frac{\lambda}{\beta_2} + \frac{\lambda}{\beta_2} e^{(q_2-1)\beta_2 x}\right)^{\frac{1}{1-q_2}}$$

Diagram labels for the equation above:

- First normalization factor (points to A)
- Second normalization factor (points to $(1 - A)$)
- First entropic index (points to q_1)
- Second entropic index (points to q_2)
- First inverse temperature (points to β_1)
- Second inverse temperature (points to β_2)

It is composed by the **sum of a first standard q -exponential function and a second function containing a further parameter $\lambda > 0$** which ensures that the total function monotonically vanishes for increasing inter-times.

A double q -exponential behavior, although kind of rare, occasionally emerges in **complex systems** (nucleotide inter-distances in DNA sequences of Homo Sapiens)

Details of the fitting parameters for the eight samples considered

Sample	A	β_1	q_1	β_2	q_2	λ
AG-5 MPa	0.975	3.5	1.48	0.01	1.7	0.09
AG-10 MPa	0.98	2.0	1.32	0.02	2.5	0.19
AG-20 MPa	0.98	1.3	1.2	0.04	2.0	0.13
AG-40 MPa	0.983	2.6	1.16	0.017	1.4	0.12
DDS-5 MPa	0.975	1.5	1.4	0.0001	1.7	0.055
DDS-10 MPa	0.98	4.0	1.32	0.02	1.7	0.19
DDS-20 MPa	0.98	4.1	1.24	0.017	1.5	0.20
DDS-40 MPa	0.983	4.6	1.16	0.015	2.4	0.19

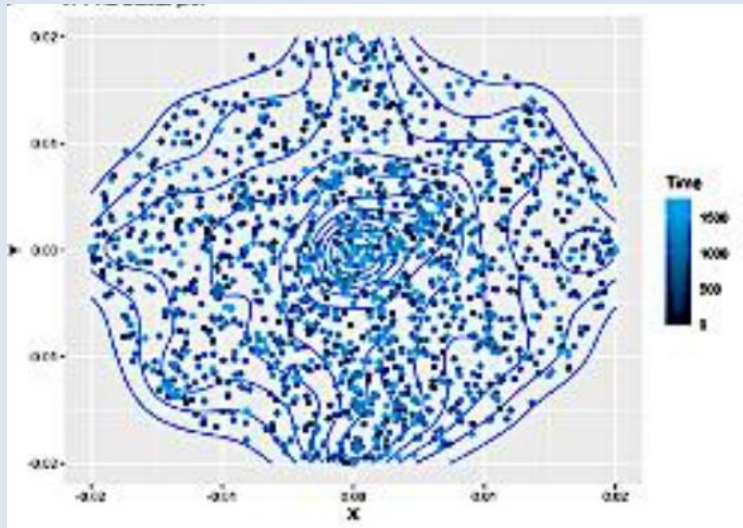
For any material and confinement, typically $\beta_1 \gg \beta_2$ and $q_1 < q_2$.

Moreover, in correspondence of the same amount of confinement, values of A coincide for AG and DDS.

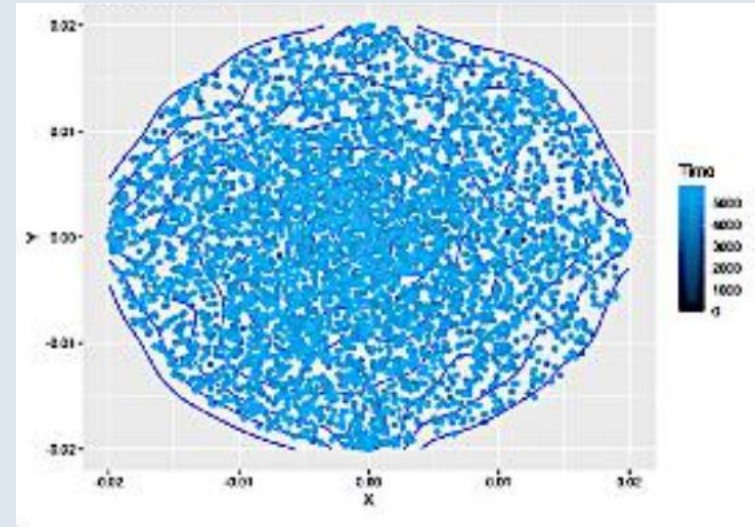
AE Positions in space

Subsequent positions expressed in meters, ordered in time before breakdown (with a blue scale of decreasing intensity) are projected on the three planes X-Y, X-Z and Y-Z

Examples of Scatter Plots



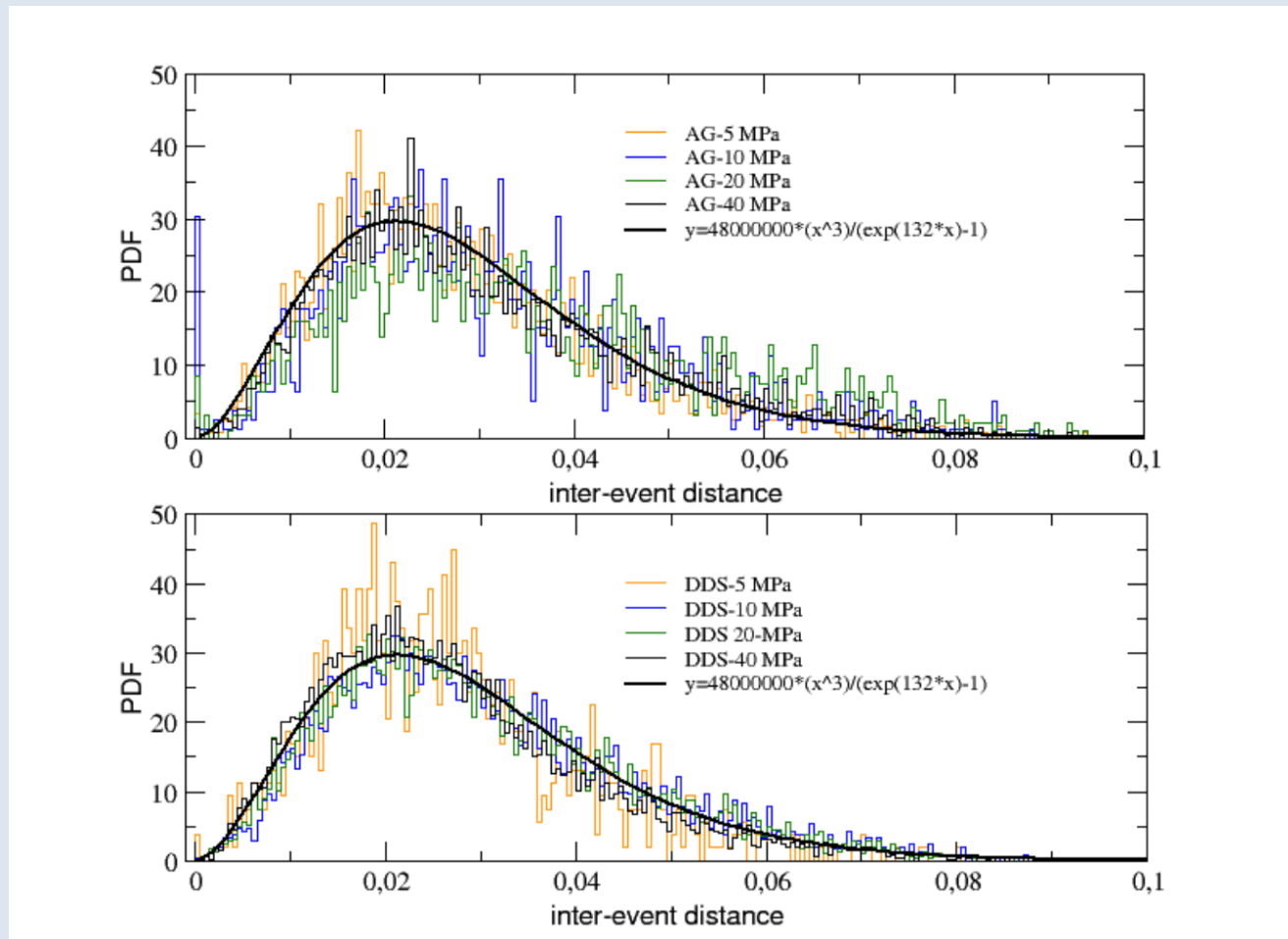
AG-10 MPa
X-Y plane



DDS 10-MPa
X-Y plane

Spatial distributions of AE show a **higher clustering of events in AG**, where fracturing occurs throughout localized planar fractures, while **more scattered nucleation centers** related to dilatant patches occur prior failure in DDS.

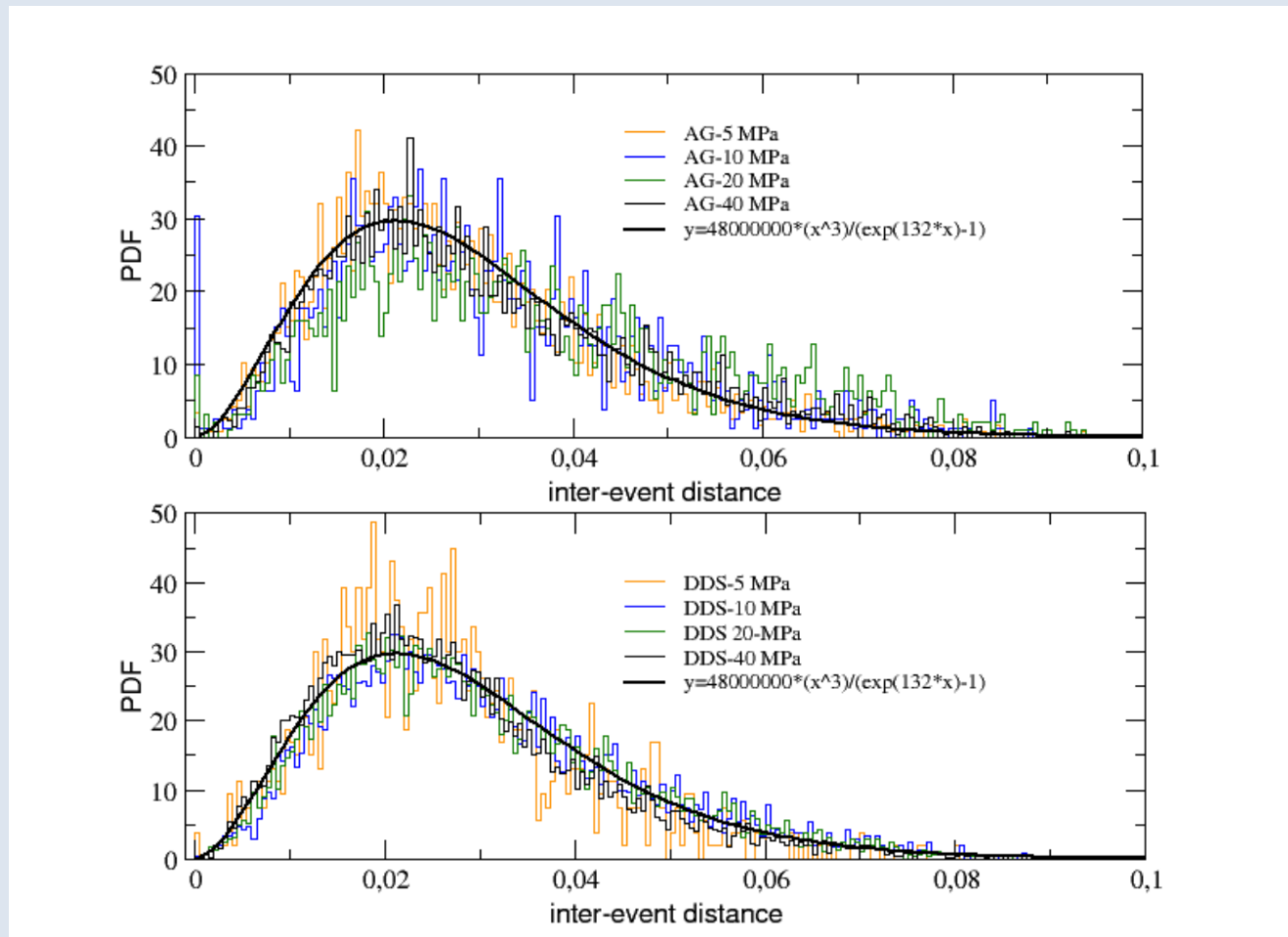
PDFs of AE inter-event distances



AE inter-event distances are defined as the **metric distance between the 3D spatial positions of two subsequent recorded AE events** inside a given sample during an experiment

$$d(n) = \sqrt{[x_{AE}(n) - x_{AE}(n-1)]^2 + [y_{AE}(n) - y_{AE}(n-1)]^2 + [z_{AE}(n) - z_{AE}(n-1)]^2}$$

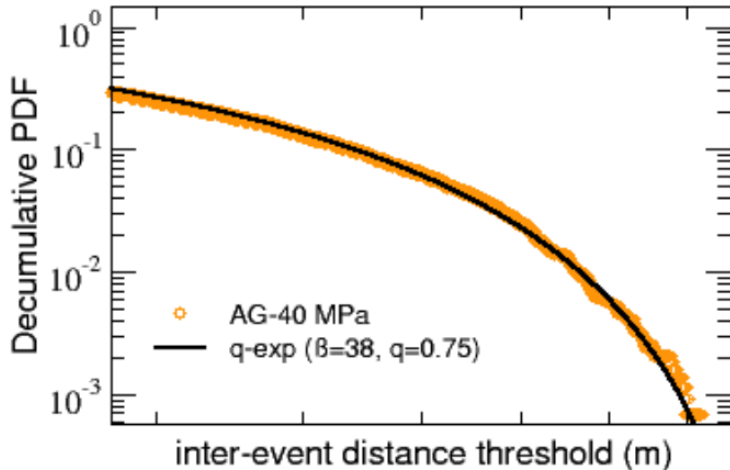
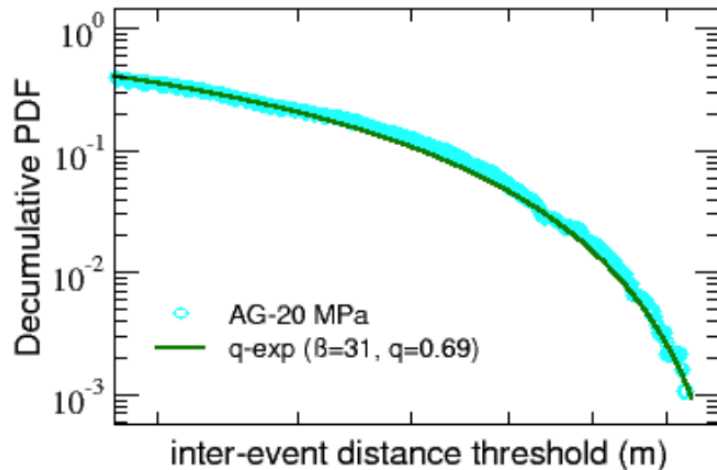
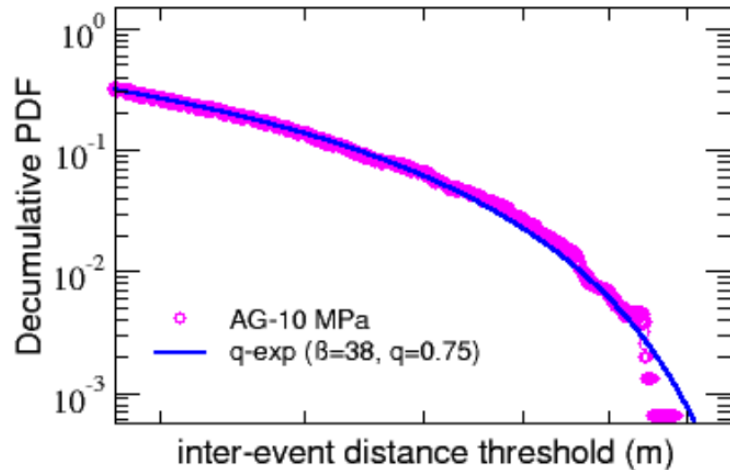
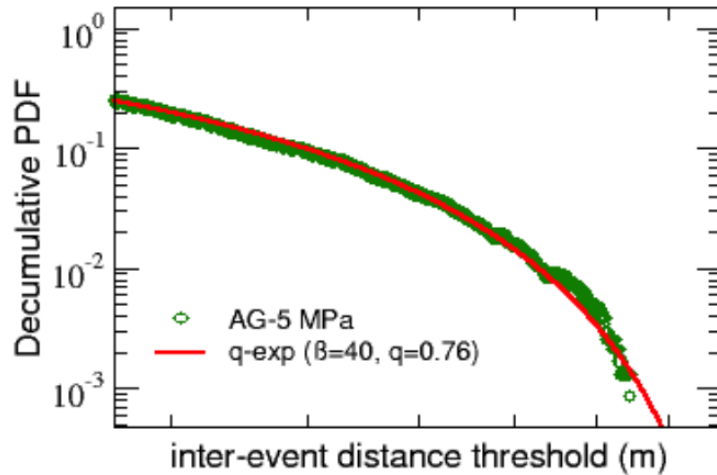
PDFs of AE inter-event distances



Planck-like distribution, with a maximum and an asymmetric tail, which can be well fitted by the following function:
$$y = \frac{A x^3}{e^{Bx} - 1}$$

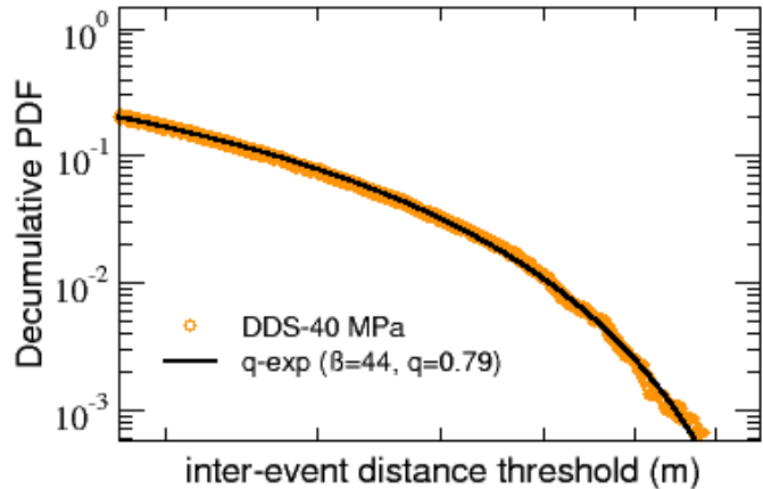
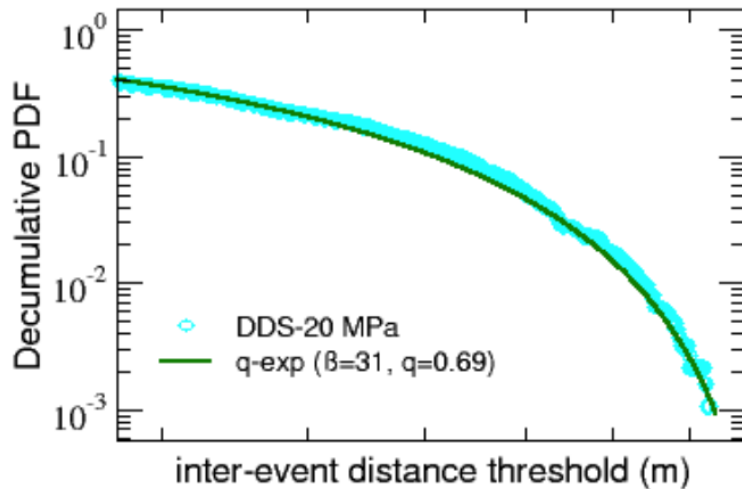
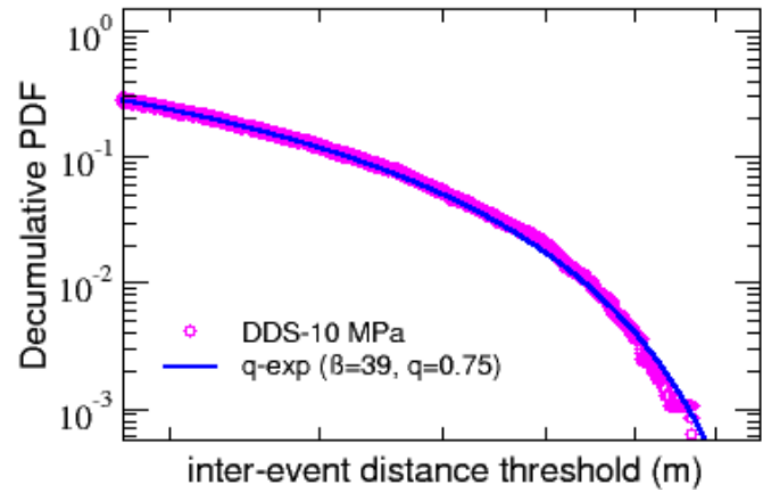
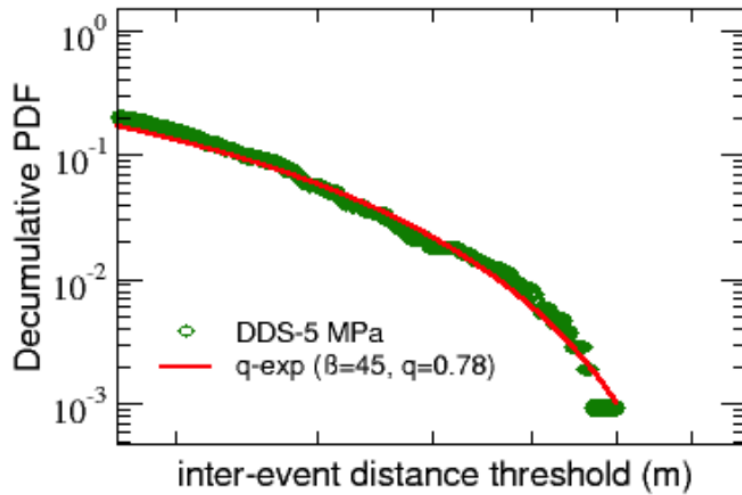
where the values of the two fitting parameters ($A = 4.8 \cdot 10^7$ and $B = 132$) are **independent of the type of materials and of the confinement**, thus revealing again some kind of **universal behavior**

Decumulative distributions $P(> d)$ of the inter-event distances



In this case it is possible to fit all the distributions with **single standard q-exponential functions** with inverse temperature β and an entropic index q which is always smaller than 1, indicating not a power law behavior but revealing the presence of a cut-off in the distributions

Decumulative distributions $P(> d)$ of the inter-event distances



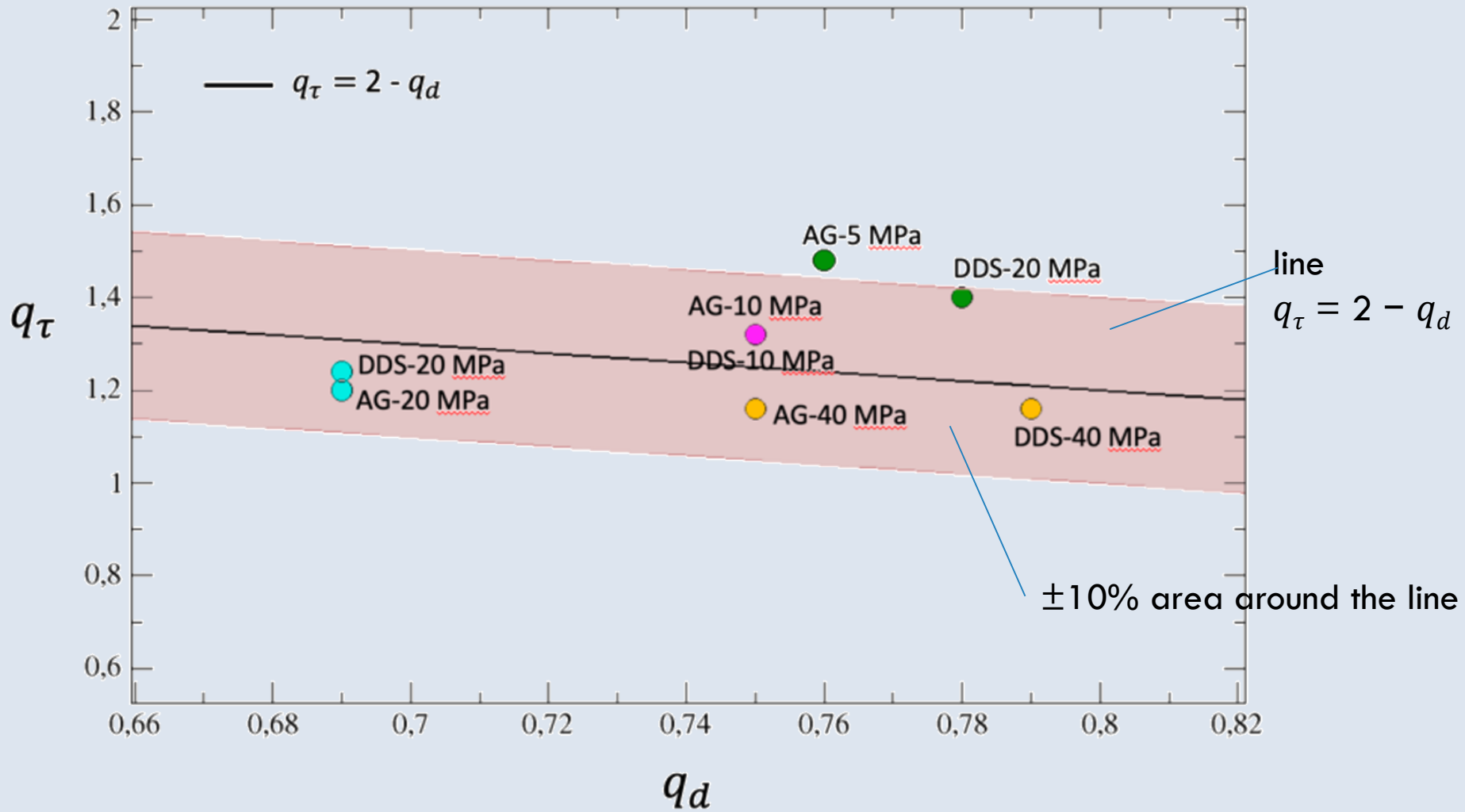
In this case it is possible to fit all the distributions with **single standard q-exponential functions** with inverse temperature β and an entropic index q which is always smaller than 1, indicating not a power law behavior but revealing the presence of a cut-off in the distributions

Entropic indices q_τ and q_d

Sample	q_τ	q_d	$q_\tau + q_d$
AG-5 MPa	1.48	0.76	2.24
AG-10 MPa	1.32	0.75	2.07
AG-20 MPa	1.2	0.69	1.89
AG-40 MPa	1.16	0.75	1.91
DDS-5 MPa	1.4	0.78	2.18
DDS-10 MPa	1.32	0.75	2.07
DDS-20 MPa	1.24	0.69	1.93
DDS-40 MPa	1.16	0.79	1.95

The sum of the entropic indices q_τ and q_d for the 8 considered samples oscillates around 2.

Entropic indices q_τ and q_d



The linear behavior holds quite well inside an error of 10% for almost all the samples

IN CONCLUSION

- Pre-failure processes in the considered materials, and in particular AE inter-event time and AE inter-event distance distributions, can be reproduced with q -exponential curves, showing universal features.
- The obtained results provide an insight on the warning signs of the incipient failure of construction materials and could therefore be used in a health monitoring strategy on existing structures.

Thank you all for your kind attention



Thank you all for your kind attention



and

Happy Birthday (again)

Constantino !

